

# **Nature Inspired Substrate-Independent Omniphobic and Antimicrobial Slippery Surfaces**

*Harrison J. Cox, Colin P. Gibson, Gary J. Sharples, and Jas Pal S. Badyal\**

Harrison J. Cox, Colin P. Gibson, Jas Pal S. Badyal

Department of Chemistry, Science Laboratories, Durham University, Durham DH1 3LE, England, UK

E-mail: [j.p.badyal@durham.ac.uk](mailto:j.p.badyal@durham.ac.uk)

Gary J. Sharples

Department of Biosciences, Science Laboratories, Durham University, Durham DH1 3LE, England, UK

Keywords: slippery surface, multifunctional, liquid repellency, omniphobic, antimicrobial, plasmachemical deposition

## ABSTRACT

Inspired by the carnivorous *Nepenthes* pitcher plant, a range of highly liquid repellent lubricant-infused surfaces have been devised (low water droplet contact angle hysteresis and sliding angle values). This entailed matching functional pulsed plasma polymer nanolayers with appropriate slippery lubricants. A molecular level structure–behaviour relationship has been developed highlighting the importance of favourable aromatic–aliphatic intermolecular interactions between coating and lubricant. Fluorinated lubricant-infused pulsed plasma polymer nanocoatings resist wetting by liquids spanning a wide range of surface tensions (including pentane, motor oil, and water, i.e. omniphobicity). In the case of natural antimicrobial compound-infused functional plasma polymer surfaces (for example the essential oil cinnamaldehyde), multifunctional performance is attained combining high liquid repellency (self-cleaning) with simultaneous strong antibacterial activity against both Gram-positive *Staphylococcus aureus* and Gram-negative *Escherichia coli* ( $\text{Log}_{10}$  Reduction > 7). In addition, these lubricant-infused functional pulsed plasma polymer surfaces easily repel a variety of everyday liquids (including foodstuffs such as tomato ketchup and honey).

## 1. INTRODUCTION

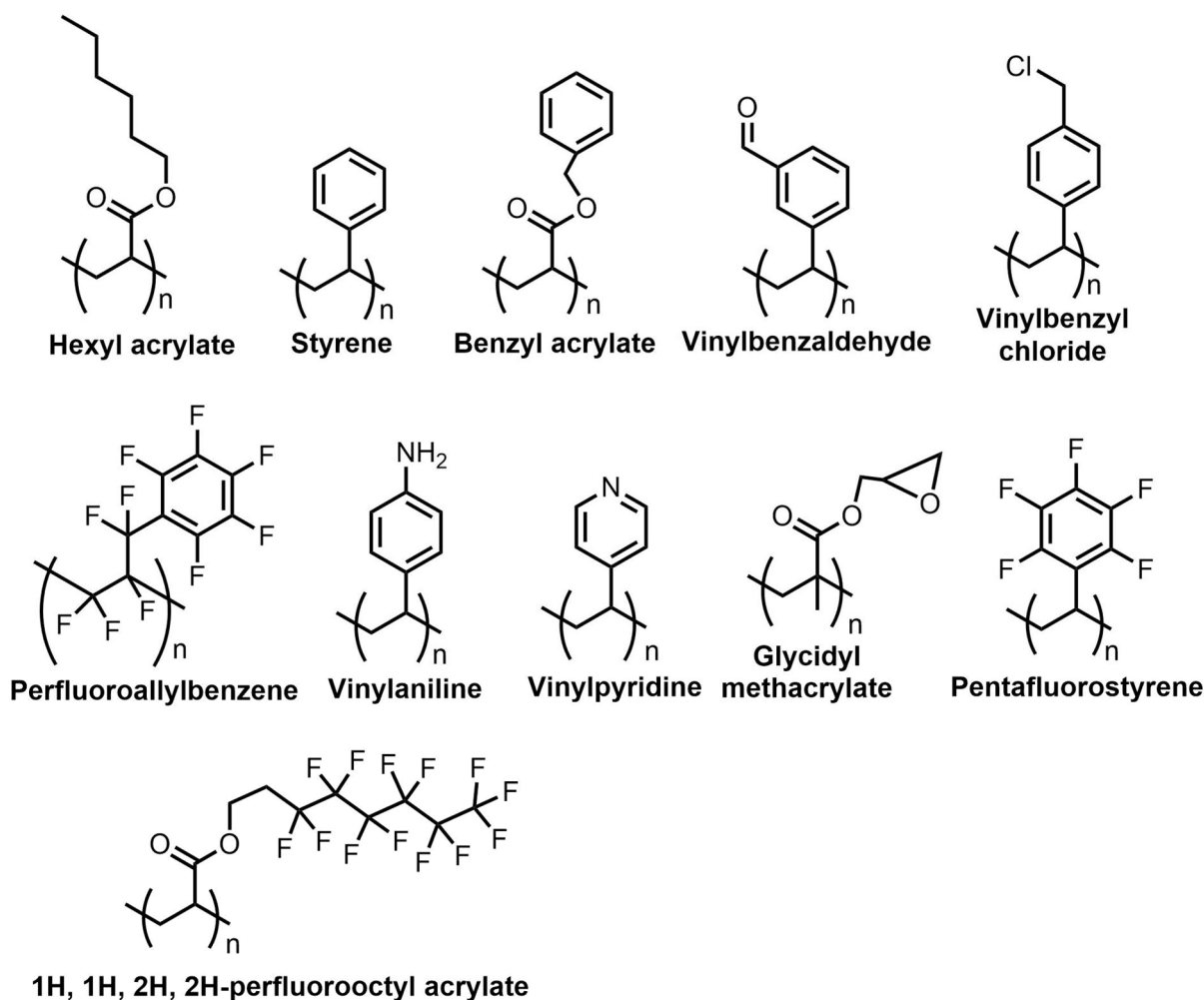
Liquid repellent slippery liquid-infused porous surfaces (SLIPS) have been inspired by the carnivorous *Nepenthes* pitcher plant, in which a nectar film entrapped within a textured surface on the plant peristome is used to attract and capture arthropod prey.<sup>[1]</sup><sup>[2]</sup><sup>[3]</sup><sup>[4]</sup><sup>[5]</sup> In the past, SLIPS have been fabricated by impregnating a roughened or porous surface with a lubricating liquid. The lubricant must be able to wet and adhere to the host surface in preference to the liquid which is being repelled, and the lubricant needs to be immiscible with the liquid being repelled. This can be achieved through careful matching of the solid surface and lubricant chemistries. Slippery lubricant-infused surfaces have been proposed for a wide variety of technological and societal applications including: water repellency,<sup>[5]</sup> antibacterial,<sup>[6]</sup> marine antibiofouling,<sup>[7]</sup> blood repellency,<sup>[8]</sup> icephobicity,<sup>[9]</sup> anti-icing,<sup>[10]</sup> corrosion resistance,<sup>[10]</sup> mineral fouling mitigation,<sup>[11]</sup> droplet motion control,<sup>[12]</sup> water harvesting,<sup>[13]</sup> fog collection,<sup>[14]</sup> antireflectivity,<sup>[15]</sup> antifouling of foodstuffs,<sup>[16]</sup> antifouling of faecal matter,<sup>[17]</sup> underwater bubble transportation,<sup>[18]</sup> and drag reduction.<sup>[19]</sup> Prevention of bacterial biofilm formation and surface fouling are of considerable societal importance, particularly in the healthcare and medical settings (for example, the vast majority of catheter-associated urinary tract infections are caused by biofilms formed on the catheters).<sup>[20]</sup> In the marine environment on the hulls of ships, bacterial biofilm formation and fouling results in increased frictional drag, which leads to more fuel consumption and greater greenhouse gas emissions.<sup>[21]</sup> Bacterial biofilms are also of concern in the food industry, given their role in food spoilage and risks to public health.<sup>[22]</sup> Therefore, eco-friendly lubricant-infused slippery surfaces are potential candidates for tackling a wide range of societal and environmental issues.

In the absence of any bactericidal additives, SLIPS do not possess the ability to kill bacteria.<sup>[23]</sup> Therefore typically an antimicrobial agent (for example drug molecules such as triclosan<sup>[24]</sup>) needs to be impregnated into a pre-made SLIPS, or silver is incorporated into the substrate prior to lubricant infusion.<sup>[25]</sup> However, environmental concerns exist about the toxicity of triclosan towards marine life, as well as its bioaccumulation, and the risk for bacteria to develop antimicrobial resistance towards the drug.<sup>[26]</sup> Whereas silver (and silver compounds) typically have high costs when compared to organic compounds, and again there is concern about the

emergence of antimicrobial resistance,<sup>[27]</sup> as well as toxicity towards the environment and humans.<sup>[28],[29]</sup> Furthermore, many of the reported fabrication techniques for SLIPS systems are limited in the range and geometries of materials that they can be produced on. For example, hydrothermal treatment is applicable to inorganic surfaces such as aluminium and glass,<sup>[30], [31]</sup> whilst electroplating is restricted to metals,<sup>[32]</sup> and the use of inherently porous or micro/nanostructured materials to infiltrate lubricants cannot be extended to non-porous materials.<sup>[33]</sup> In the case of layer-by-layer deposition techniques, typically long coating times are required to build up a sufficient coating layer thickness.<sup>[34]</sup> Also, these methodologies require multiple steps, and often need an extra substrate hydrophobization step in order to provide sufficient surface affinity towards the lubricant impregnation.<sup>[30],[31],[32],[33],[34]</sup>

In this article, a simple and quick two-step coating method is described, comprising conformal pulsed plasma polymerisation of a variety of functional monomers onto solid substrates, followed by lubricant impregnation into the deposited functional nanolayer to produce slippery lubricant-infused surfaces, Scheme 1. Pulsed plasmachemical deposition entails two distinct reaction regimes: the short period on-time ( $t_{on}$ —typically microseconds, where electrical discharge ignition leads to the formation of initiator radical species from the monomer) and then the longer period off-time ( $t_{off}$ —typically milliseconds, where conventional stepwise addition chain-growth monomer polymerisation proceeds).<sup>[35],[36]</sup> This culminates in excellent structural retention of the monomer functional groups to yield well-defined functional polymer nanocoatings.<sup>[35]</sup> Key advantages of pulsed plasmachemical surface functionalisation include a simple and quick single-step process, ambient temperature, conformal 3-dimensional coating, independent of substrate material, excellent adhesion, solventless, minimal waste, and low energy consumption. Such dry coating processes are scalable and capable of reaching roll-to-roll line speeds of several hundred metres per minute.<sup>[37]</sup> A variety of different functional monomers have been utilised to prepare a range of pulsed plasma deposited nanolayer surface chemistries for compatibilization with appropriate functional lubricants to yield a structure–behaviour relationship for slippery surface fabrication, Structures 1 and Structures 2. Further fine tuning (molecular tailoring) of the surface compatibilization properties can be achieved by varying the pulsed plasma duty cycle parameters.





Structures 2. Chemical structures of pulsed plasma functional nanolayers and associated monomer names.

Lubricants employed include: environmentally-friendly cinnamaldehyde (a major component of cinnamon tree bark oil<sup>[38]</sup>—which displays potent broad-spectrum antibacterial activity,<sup>[39]</sup> as well as antiviral,<sup>[40]</sup> and antifungal<sup>[41]</sup> efficacies); citral (present in the oils of lemon (*Citrus limon*), sweet orange (*Citrus sinensis*), and bergamot (*Citrus bergamia*)<sup>[42]</sup>); decanal (contained in the oils of sweet orange (*Citrus sinensis*), and coriander leaf (*Coriandrum sativum* L.)<sup>[43], [44]</sup>); and 2-methylundecanal (found in the essential oils extracted from members of the Rutaceae family (including *Ruta graveolens*<sup>[45]</sup>), Structures 1. Cinnamaldehyde, citral, and decanal lubricants are all classified as, ‘generally recognised as safe’ (GRAS) by the US Food and Drug Administration,<sup>[46]</sup> and 2-methylundecanal does not present a safety concern to human health according to the Joint FAO/WHO Expert Committee on Food Additives

(JECFA).<sup>[47]</sup> Other lubricants investigated include hexadecane (as a non-polar lubricant) and fluorinated lubricants (perfluorotributylamine, perfluoropolyether and perfluorodecalin). A molecular level structure–behaviour relationship has been developed for the fabrication of slippery surfaces by comparing the liquid repellency between different combinations of functional pulsed plasma nanocoating and impregnated lubricant liquid, Structures 1 and Structures 2.

## 2. RESULTS

### 2.1 Control Studies

Water contact angle hysteresis and sliding angle values for uncoated PET film substrate and following treatment with each of the lubricants were all measured to be relatively large in magnitude, Table 1 and Supporting Information Table S 1.

Table 1. Water droplet static, advancing, receding, and hysteresis contact angle values, and water droplet sliding angle values, for coated PET film substrates. Values are reported as mean  $\pm$  standard deviation. \* Water droplet showed no movement at 90° inclination of substrate from the horizontal. † Cinnamaldehyde dissolves poly(styrene), and so it is not possible to prepare slippery surfaces for this combination.

Surface	Contact Angle / °		Sliding Angle / °
	Static	Hysteresis	
PET Untreated	66.8 $\pm$ 1.6	52 $\pm$ 4	48 $\pm$ 2
Pulsed Plasma Poly(hexyl acrylate)	82.2 $\pm$ 0.8	8.5 $\pm$ 1.1	10.7 $\pm$ 0.5
Pulsed Plasma Poly(styrene) (ppPS)	79 $\pm$ 2	29 $\pm$ 10	37 $\pm$ 1
ppPS–Decanal	82.5 $\pm$ 0.7	9 $\pm$ 7	1.3 $\pm$ 0.2
ppPS–Hexadecane	98.6 $\pm$ 0.4	0.8 $\pm$ 0.5	1.0 $\pm$ 0.0
ppPS–2-Methylundecanal	68.8 $\pm$ 1.6	3 $\pm$ 3	1.7 $\pm$ 0.2
ppPS–Cinnamaldehyde	89 $\pm$ 4	37 $\pm$ 11	39 $\pm$ 1
Drop-Cast Poly(styrene) (dcPS)	90.3 $\pm$ 1.0	20 $\pm$ 3	14 $\pm$ 1
dcPS–Hexadecane	87.9 $\pm$ 1.0	5 $\pm$ 3	3 $\pm$ 1
Petri Dish Poly(styrene) (pdPS)	88.8 $\pm$ 1.1	30 $\pm$ 2	25 $\pm$ 1
pdPS–Hexadecane	94.7 $\pm$ 0.5	6 $\pm$ 3	6.7 $\pm$ 0.5
pdPS–Cinnamaldehyde †	-	-	-
Pulsed Plasma Poly(benzyl acrylate) (ppBA)	72.4 $\pm$ 0.6	30 $\pm$ 2	37.7 $\pm$ 0.5
ppBA–Decanal	56.1 $\pm$ 0.5	2 $\pm$ 4	2.7 $\pm$ 0.5
ppBA–Hexadecane	85 $\pm$ 2	21 $\pm$ 2	14 $\pm$ 0
ppBA–2-Methylundecanal	66 $\pm$ 1	0.5 $\pm$ 0.4	2 $\pm$ 0
ppBA–Cinnamaldehyde	60 $\pm$ 2	4 $\pm$ 4	3.3 $\pm$ 0.5

Pulsed Plasma Poly(vinylbenzaldehyde) (ppVBA)	70.2 ± 1.5	38 ± 8	44 ± 1
ppVBA–Decanal	35.3 ± 0.7	5.9 ± 1.2	4 ± 1
ppVBA–Hexadecane	74 ± 2	1 ± 2	17 ± 1
ppVBA–2-Methylundecanal	67.6 ± 0.1	2.6 ± 1.6	1.7 ± 0.2
ppVBA–Cinnamaldehyde	58 ± 3	2.3 ± 1.2	13 ± 1
Pulsed Plasma Poly(vinylbenzyl chloride) (ppVBC)	84.4 ± 0.5	18 ± 2	14 ± 1
ppVBC–Decanal	54 ± 3	3 ± 4	6.8 ± 0.2
ppVBC–Hexadecane	81 ± 3	2 ± 3	15 ± 1
ppVBC–2-Methylundecanal	67 ± 2	1 ± 4	1 ± 0
ppVBC–Cinnamaldehyde	67 ± 3	9 ± 3	27 ± 1
Pulsed Plasma Poly(perfluoroallylbenzene) (ppPFAB)	97 ± 2	23 ± 4	30 ± 1
ppPFAB–Perfluorotriethylamine	118.4 ± 0.4	2.6 ± 0.9	2.7 ± 0.5
ppPFAB–Perfluoropolyether	109 ± 3	3.8 ± 3.8	1.7 ± 0.2
ppPFAB–Perfluorodecalin	119.1 ± 0.5	18 ± 5	9 ± 1
Pulsed Plasma Poly(vinylaniline) (ppVA)	75 ± 6	66 ± 3	90 (*)
ppVA–Decanal	72.6 ± 0.9	4.6 ± 1.6	13 ± 1
ppVA–Hexadecane	75.4 ± 0.3	5.3 ± 1.6	17 ± 1
ppVA–2-Methylundecanal	80.0 ± 1.4	8.8 ± 1.3	14 ± 2
ppVA–Cinnamaldehyde	56.6 ± 0.1	2.8 ± 1.0	10 ± 1
ppVA–Citral	67.3 ± 0.6	1.7 ± 0.3	12 ± 2

Pulsed plasma deposition covering a range of functional monomers was undertaken to provide a variety of well-adhered conformal host layers for lubricant impregnation, Structures 2, Table 1, and Supporting Information Table S 2. In the case of pulsed plasma deposited poly(vinylpyridine), poly(glycidyl methacrylate), poly(pentafluorostyrene), and poly(1H, 1H, 2H, 2H, perfluorooctyl acrylate), all were found to produce non-slippery surfaces when treated with the selection of test lubricants, Supporting Information Figure S 1, Figure S 2, Figure S 3, Figure S 4, Table S 3, Table S 4, Table S 5 and Table S 6.

## 2.2 Pulsed Plasma Poly(Hexyl Acrylate)

Hexyl acrylate monomer displays the following characteristic infrared absorption bands: C–H stretching ( $3000\text{--}2830\text{ cm}^{-1}$ ), acrylate carbonyl C=O stretching ( $1724\text{ cm}^{-1}$ ), acrylate C=C stretching ( $1638\text{ cm}^{-1}$  and  $1631\text{ cm}^{-1}$ ), and the C–O ester stretch ( $1182\text{ cm}^{-1}$ ), Supporting Information Figure S 5.<sup>[48]</sup> Pulsed plasma deposited poly(hexyl acrylate) shows loss of the acrylate carbon–carbon double bond infrared absorbance features, thereby confirming that polymerisation had taken place.<sup>[35]</sup>

AFM roughness measurements showed that the pulsed plasma poly(hexyl acrylate) coating surface is not significantly more rough compared to uncoated silicon wafer substrate ( $Roughness_{RMS} = 1.99$  nm versus 0.68 nm respectively for 10  $\mu$ m scan size)—which is typical of low duty cycle pulsed plasma deposited polymer nanocoatings, Figure 1.<sup>[49],[50]</sup>

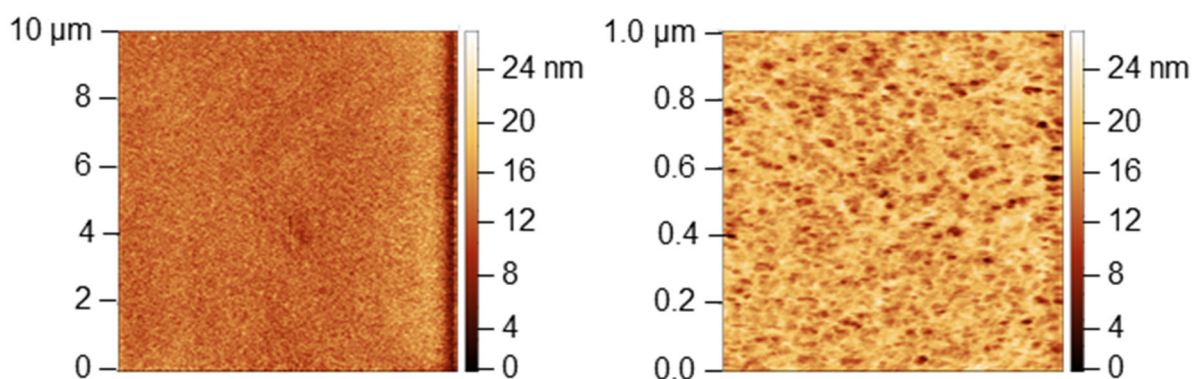


Figure 1. Atomic force microscopy (AFM) images of pulsed plasma poly(hexyl acrylate) coated silicon wafer.

Pulsed plasma polymerised hexyl acrylate coatings displayed relatively small water contact angle hysteresis ( $<10^\circ$ ) and sliding angle ( $\sim 10^\circ$ ) values, Table 1. This may be attributed to either the relative flatness of the surface or weak (liquid-like) interactions between neighbouring surface alkyl chains.<sup>[51]</sup> None of the lubricant liquids tested significantly lowered the water contact angle hysteresis value, Supporting Information Table S 7.

### 2.3 Pulsed Plasma Poly(Styrene)

Liquid styrene monomer exhibits the following characteristic infrared absorption bands: C–H stretching ( $3100\text{--}2965$   $\text{cm}^{-1}$ ), aromatic ring summations ( $2000\text{--}1700$   $\text{cm}^{-1}$ ), vinyl C=C stretch ( $1629$   $\text{cm}^{-1}$ ), aromatic C=C stretching ( $1600$   $\text{cm}^{-1}$ ,  $1574$   $\text{cm}^{-1}$ ,  $1494$   $\text{cm}^{-1}$ , and  $1448$   $\text{cm}^{-1}$ ),  $\text{CH}_2$  deformations ( $1412$   $\text{cm}^{-1}$ ), HC=CH trans wag ( $994$   $\text{cm}^{-1}$ ), and = $\text{CH}_2$  wag ( $906$   $\text{cm}^{-1}$ ), Supporting information Figure S 6.<sup>[52]</sup> The vinyl group bands were absent in the deposited pulsed plasma poly(styrene) infrared spectrum, indicating that polymerisation has taken place. Whilst aromatic ring features are still present, thereby confirming structural retention of the phenyl rings.

Pulsed plasma deposited poly(styrene) on PET substrate displays a large water contact angle hysteresis, Table 1. Whereas a slippery surface was obtained following decanal, 2-methylundecanal, or hexadecane impregnation into the pulsed plasma poly(styrene) coating. Hexadecane lubricant in particular gave excellent water-repellent properties, with both contact angle hysteresis and sliding angle values measured to be  $\leq 1^\circ$ . Cinnamaldehyde and perfluorotributylamine lubricants did not form a slippery surface when combined with the poly(styrene) coating.

In order to determine whether this approach for making slippery lubricant-infused surfaces could be extended beyond pulsed plasma deposited poly(styrene) coatings, conventional poly(styrene) coatings were drop-cast onto glass slides and treated with hexadecane lubricant. This led to a significant reduction of both the water contact angle hysteresis and the sliding angle values ( $\leq 5^\circ$ ), thereby demonstrating that the drop-cast poly(styrene) films also form slippery lubricant-infused surfaces, Table 1. Pre-formed poly(styrene) pieces cut from Petri dishes and then treated with hexadecane behaved in a similar fashion. Henceforth, a range of aromatic ring containing pulsed plasma polymer coatings were investigated and shown to provide slippery surfaces following impregnation with lubricants—these included pulsed plasma deposited poly(benzyl acrylate), poly(vinylbenzaldehyde), poly(vinylbenzyl chloride), poly(perfluoroallylbenzene), and poly(vinylaniline), Structures 2, Table 1, and Supporting Information Figure S 7, Figure S 8, Figure S 9, and Table S 8

#### **2.4 Pulsed Plasma Poly(Perfluoroallylbenzene)**

Perfluoroallylbenzene monomer displays the following characteristic infrared absorption bands: allyl C=C stretch ( $1787\text{ cm}^{-1}$ ), aromatic C–C stretching ( $1657\text{ cm}^{-1}$ ,  $1528\text{ cm}^{-1}$ , and  $1502\text{ cm}^{-1}$ ), Supporting Information Figure S 10.<sup>[53]</sup> It is difficult to unambiguously assign features in the spectral region below  $1400\text{ cm}^{-1}$ , but peaks in this region are typically characteristic of C–F stretching vibrational modes.<sup>[54]</sup> Following pulsed plasma deposition, the allyl bond diminished in intensity (which is consistent with polymerisation taking place). Retention of the aromatic stretching bands in the pulsed plasma deposited layer confirms structural retention of the perfluorinated phenyl rings in the coating.<sup>[53]</sup>

Pulsed plasma poly(perfluoroallylbenzene)-only coating did not display low water contact angle hysteresis or water sliding angle values, Table 1. Both

perfluorotributylamine and perfluoropolyether infused surfaces yielded coatings with low water contact angle hysteresis and sliding angle values ( $< 5^\circ$ ). In order to demonstrate omniphobicity (low contact angle hysteresis / sliding angle towards both polar and non-polar liquids), the perfluorotributylamine-infused surface was able to resist wetting by heptane (surface tension =  $20.14 \text{ mN m}^{-1}$ ).<sup>[55]</sup> Whilst, the perfluoropolyether-infused surface coating resisted wetting by pentane (surface tension =  $15.8 \text{ mN m}^{-1}$ ), as well as heptane, vacuum pump oil, and engine oil all slide off at low angles ( $< 17 \pm 1^\circ$ ,  $2.3 \pm 0.2^\circ$ , and  $2.2 \pm 0.2^\circ$  respectively). For the case of perfluorodecalin infused surface, both the water contact angle hysteresis and sliding angle values were lowered.

## 2.5 Pulsed Plasma Poly(Vinylaniline)

The characteristic infrared bands of vinylaniline monomer can be assigned as follows: asymmetric amine stretch ( $3440 \text{ cm}^{-1}$ ), symmetric amine stretch ( $3370 \text{ cm}^{-1}$ ), aromatic C–H stretch ( $3100\text{--}3000 \text{ cm}^{-1}$ ), ring summations ( $2000\text{--}1750 \text{ cm}^{-1}$ ), vinyl C=C stretch ( $1622 \text{ cm}^{-1}$ ),  $\text{NH}_2$  deformations ( $1610 \text{ cm}^{-1}$ ), para-substituted aromatic ring stretch ( $1513 \text{ cm}^{-1}$ ),  $=\text{CH}_2$  deformations ( $1412 \text{ cm}^{-1}$ ), aromatic C–N stretch ( $1314 \text{ cm}^{-1}$ ), para-substituted benzene ring stretch ( $1177 \text{ cm}^{-1}$ ), HC=CH trans wag ( $994 \text{ cm}^{-1}$ ),  $=\text{CH}_2$  wag ( $893 \text{ cm}^{-1}$ ), and  $-\text{NH}_2$  wag ( $830 \text{ cm}^{-1}$ ), Supporting Information Figure S 11.<sup>[56]</sup> Pulsed plasma deposited poly(vinylaniline) shows similar infrared absorption bands, apart from the disappearance of the vinyl C=C group features ( $1622 \text{ cm}^{-1}$  and  $994 \text{ cm}^{-1}$ ) and the appearance of an aliphatic C–H stretch ( $2865 \text{ cm}^{-1}$ ) confirming that polymerisation has taken place.<sup>[56]</sup>

Pulsed plasma poly(vinylaniline)-coated PET substrates display large water contact angle hysteresis and sliding angle values (water droplet showed no movement at  $90^\circ$  inclination of the substrate from the horizontal), Table 1. Following impregnation with decanal, 2-methylundecanal, hexadecane, cinnamaldehyde, or citral lubricants, low water contact angle hysteresis and sliding angle values were measured. The citral-infused surface gave rise to the lowest water contact angle hysteresis value ( $1.7 \pm 0.3^\circ$ ), and cinnamaldehyde-infused surface produced the lowest water sliding angle ( $10 \pm 1^\circ$ ). The slippery behaviour displayed by the hexadecane-infused surface indicates that the pulsed plasma poly(vinylaniline) coating is also compatible with non-

polar lubricants. Perfluorotributylamine did not form a slippery surface when combined with the pulsed plasma poly(vinylaniline) coating.

Decanal, 2-methylundecanal, cinnamaldehyde, and citral, lubricant-infused surfaces were left to stand for 4 months under ambient open-air laboratory conditions. Decanal and 2-methylundecanal lubricant-infused surfaces continued to display slippery behaviour after this 4-month storage period. Given that the contact angle technique is highly surface-sensitive, this demonstrates that the lubricants remain stable, otherwise there would be a change in contact angle values. It was found that the cinnamaldehyde and citral lubricant-infused surfaces no longer showed any slippery behaviour towards water droplets (probably due to essential oil evaporation). However, these slippery surfaces could easily be regenerated by immersion for 5 min in the corresponding essential oil. Less volatile essential oil molecules should give rise to even longer shelf-lives for these lubricant-impregnated surfaces.

The coatings' slippery performance was tested further using real-world foodstuffs. Tomato ketchup filled into an untreated glass vial showed no movement at all during gentle shaking, and when the vial was inverted, some of the ketchup fell out but much of it remained stuck to the insides of the vial, Supporting Information Video S 1. Control uncoated glass vials were also rinsed with just the lubricant aldehydes (decanal, 2-methylundecanal cinnamaldehyde, and citral). For the decanal control vial, some very slow ketchup movement was observed over the course of 50 s, Figure 2 and Supporting Information Video S 2. Shaking the vial removed some ketchup, although much still remained. No ketchup movement was observed for the 2-methylundecanal control vial, and shaking the vial left much ketchup stuck to the walls of the vial. Cinnamaldehyde and citral control vials showed increased ketchup movement compared to the untreated vial, with some ketchup sliding out of the vial without any need to shake it. However, there remained ketchup in the vial which stopped moving after approximately 30 s. For decanal, 2-methylundecanal, and cinnamaldehyde infused pulsed plasma poly(vinylaniline) coated glass vial surfaces, the ketchup readily slid out of the vial as soon as it was flipped over, with all the ketchup having left the vial in about 5 s, Figure 2 and Supporting Information Video S 3. For citral-infused coating, the ketchup remained in place for approximately 5 s after the vial was upturned, and then started to slide out. Most of the ketchup left the vial, but some was still visible on the side.

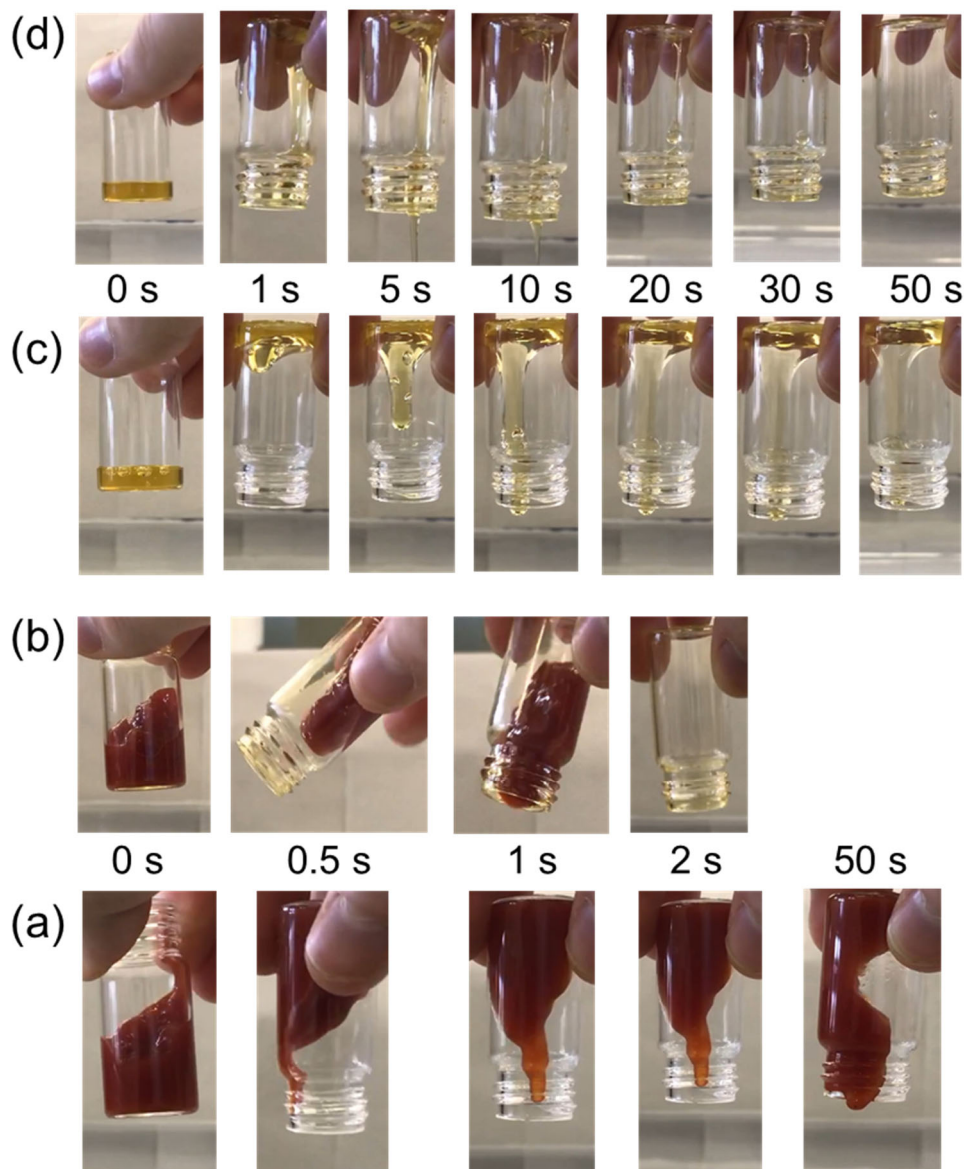


Figure 2. Time lapse photographs of: (a) ketchup applied to glass vial rinsed with decanal (control), Supporting Information Video S 2; (b) ketchup applied to pulsed plasma poly(vinylaniline) coated glass vial impregnated with decanal lubricant, Supporting Information Video S 3; (c) honey applied to glass vial rinsed with 2-methylundecanal (control), Supporting Information Video S 5; and (d) honey applied to pulsed plasma poly(vinylaniline) coated glass vial impregnated with 2-methylundecanal lubricant, Supporting Information Video S 6.

In the case of honey placed into an untreated glass vial, the honey started to run slowly down the wall of the vial over the course of a minute or so, and several drops exited the vial, Supporting Information Video S 4. The rate at which the honey subsequently came out slowed down, and a relatively large amount of content was left behind attached to the bottom and sides of the vial. Similarly, for honey placed into the aldehyde lubricant rinsed control glass vials (decanal, 2-methylundecanal

cinnamaldehyde, and citral), the honey flowed slowly with a significant amount remaining behind, Figure 2 and Supporting Information Video S 5. The movement of honey in the vials coated with lubricant-infused pulsed plasma poly(vinylaniline) surfaces (decanal, 2-methylundecanal, cinnamaldehyde, and citral) was significant, leading to the majority of the honey leaving the vials (with the exception of a few small droplets) over the same timeframe as the controls, Figure 2 and Supporting Information Video S 6. Prior to commercialisation, pulsed plasma poly(vinylaniline) would be tested by the relevant national food safety agency; whilst for example analogous poly(styrene) based slippery surfaces, the use of poly(styrene) is already approved for food safety by the US Food and Drug Administration (FDA).<sup>[57]</sup>

Cinnamaldehyde-infused pulsed plasma poly(vinylaniline) coated PET film surfaces were tested for antibacterial activities against Gram-negative *E. coli* and Gram-positive *S. aureus*, Figure 3 and Supporting Information Table S9. PET substrates rinsed in cinnamaldehyde-only or coated with pulsed plasma poly(vinylaniline) showed a very small effect against *E. coli* and *S. aureus* bacteria ( $\text{Log}_{10}$  Reduction < 1). This could be due to a small residual amount of cinnamaldehyde remaining on the surface after washing and drying. In contrast, the pulsed plasma poly(vinylaniline)–cinnamaldehyde coated PET substrates displayed strong antibacterial activity, giving rise to complete killing of both bacterial species with values of  $\text{Log}_{10}$  Reduction > 7—which easily exceeds the minimal  $\text{Log}_{10}$  Reduction > 3 set by the US Environmental Protection Agency Office (EPA).<sup>[58]</sup>

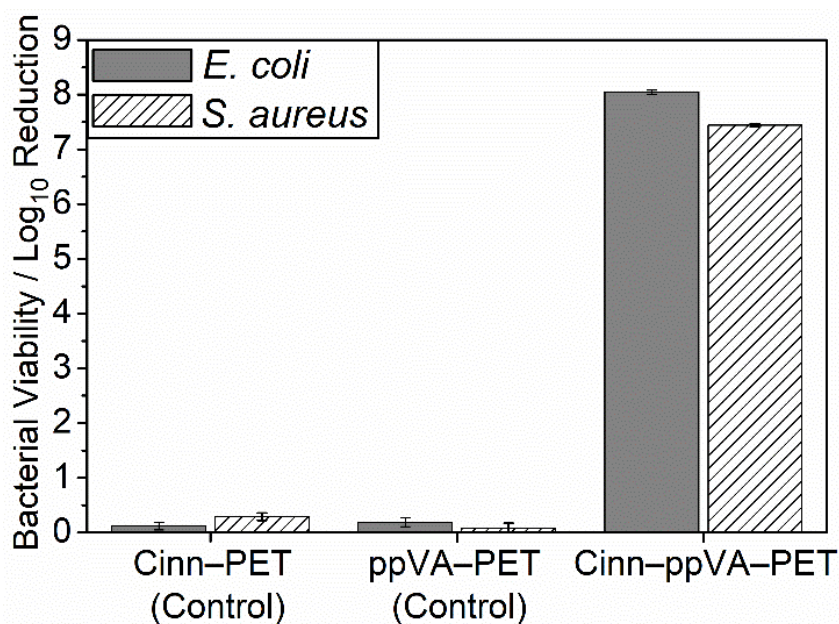


Figure 3. *E. coli* and *S. aureus* antibacterial tests for cinnamaldehyde-only treated PET (Cinn-PET, control); pulsed plasma poly(vinylaniline) coated PET (ppVA-PET, control); and pulsed plasma poly(vinylaniline)–cinnamaldehyde lubricant infused coating on PET substrate (Cinn-ppVBA-PET). Mean Log<sub>10</sub> Reduction values are relative to untreated PET substrates. Error bars represent  $\pm$  standard deviation.

Recycle testing of pulsed plasma poly(vinylaniline)–cinnamaldehyde lubricant infused surfaces against *E. coli* showed complete loss of activity on the second test (Log<sub>10</sub> Reduction (*E. coli*) =  $0 \pm 0$ ), confirming that the antibacterial mechanism corresponds to cinnamaldehyde release from the surface. Recharging the samples by repeating immersion into cinnamaldehyde again led to the complete killing of the *E. coli* (Log<sub>10</sub> Reduction (*E. coli*) =  $8.06 \pm 0.03$ ), thereby demonstrating that the coating could be easily regenerated and reused multiple times.

Pulsed plasma poly(vinylaniline) was coated onto non-woven porous polypropylene cloth, impregnated with cinnamaldehyde, and the water sliding angle values were measured (N.B. due to the dimpled surface structure of the cloth, accurate static contact angle and contact angle hysteresis values could not be measured. Therefore, only water sliding angle values are reported here), Table 2. The untreated polypropylene cloth does not show a slippery surface. After impregnation with cinnamaldehyde lubricant, the polypropylene cloth showed complete absorption/wetting by water droplets—this is likely due to the cinnamaldehyde displacing the trapped air layer in the cloth, allowing water to wick through the porous structure, but not forming a thin lubricant layer at the surface, meaning the substrate

does not repel water. The pulsed plasma poly(vinylaniline) coated polypropylene cloth exhibited a very large water sliding angle, consistent with the same coating on non-porous PET. After impregnation with cinnamaldehyde lubricant, the coating formed a slippery surface, with the water sliding angle comparable to the pulsed plasma poly(vinylaniline)–cinnamaldehyde coated PET, Table 1.

A 100  $\mu$ l droplet of high-purity water was placed onto 1.5 cm x 1.5 cm piece of pulsed plasma poly(vinylaniline)–cinnamaldehyde coated polypropylene cloth and stored in a sealed tube for 4 h. The water droplet was removed and the water sliding angle measured again—the surface remained slippery and no change was measured for the sliding angle (within error), Table 2. Another 100  $\mu$ l water droplet was dispensed onto the same sample surface and left to stand for a further 16 h (i.e. for a total water contact time of 20 h), once again, there was no change to the water droplet sliding angle. In a separate experiment, pulsed plasma poly(vinylaniline)–cinnamaldehyde coated polypropylene cloth was fully immersed into 10 ml of high purity water for 16 h, removed, and the water droplet sliding angles were measured—this also did not affect the slipperiness of the coating, and no increase to the water droplet sliding angle was observed, Table 2.

Table 2. Water droplet sliding angle values for porous polypropylene (PP) cloth substrates coated with pulsed plasma poly(vinylaniline) (ppVA) and / or cinnamaldehyde. Values are reported as mean  $\pm$  standard deviation. † Sample displays complete wetting / absorption of water droplets.

Surface	Sliding Angle / °
PP Cloth Untreated	36 $\pm$ 1
Cinnamaldehyde–PP Cloth †	-
ppVA–PP Cloth	75.3 $\pm$ 0.5
ppVA–Cinnamaldehyde	14.0 $\pm$ 0.8
ppVA–Cinnamaldehyde, 100 $\mu$ l water droplet, 4 h	13.7 $\pm$ 0.5
ppVA–Cinnamaldehyde, 100 $\mu$ l water droplet, 20 h	14.0 $\pm$ 0.8
ppVA–Cinnamaldehyde, immersion, 10 ml water, 16 h	14.7 $\pm$ 0.5

### 3. DISCUSSION

Favourable molecular level interactions of impregnated lubricants with the subsurface of non-porous flat polymer films can lead to slippery surfaces (low water contact angle

hysteresis).<sup>[16],[59],[60]</sup> This slipperiness is not due to excess lubricant remaining on the surface, and can be stable for prolonged periods of time (provided that the surface and lubricant polarities are well matched). In a similar way, functional pulsed plasma polymer coatings have been shown to form slippery surfaces by infusion of lubricants into the deposited layer, with the added advantage of being independent of substrate material and geometry, Table 1. The thickness of the pulsed plasma deposited layer is found not to be the most critical parameter, Supporting Information Table S 2. Any nanoscale porosity in the plasma deposited films will increase the effective solid–liquid interfacial area, thereby enhancing the extent of intermolecular interactions between the lubricant and pulsed plasma polymer coating. The observed dependency upon substrate coating chemical functionality confirms that the slippery behaviour is not due to excess lubricant remaining on the surface.

In terms of a structure–behaviour relationship, nonaromatic (aliphatic) pulsed plasma polymer coatings (i.e. poly(hexyl acrylate), poly(glycidyl methacrylate), and poly(1H, 1H, 2H, 2H-perfluorooctyl acrylate)) do not show a tendency to form lubricant-infused slippery surfaces, Table 1. Whereas aromatic group containing pulsed plasma polymer coatings give rise to low contact angle hysteresis and sliding angle values following lubricant application (pulsed plasma poly(styrene), drop-cast poly(styrene), Petri dish poly(styrene), pulsed plasma poly(benzyl acrylate), pulsed plasma poly(vinylbenzaldehyde), pulsed plasma poly(vinylbenzyl chloride), and pulsed plasma poly(vinylaniline)). Previous studies have shown that molecular level aromatic–aliphatic interactions can be significantly stronger than aliphatic–aliphatic and aromatic–aromatic interactions.<sup>[61],[62]</sup> It is therefore likely that the aromatic group containing plasma polymer coatings interact more strongly with the lubricants compared to the aliphatic group containing plasma polymers; this leads to lubricant infusion into the subsurface to create slippery surfaces for the former but not the latter. For the case of the aromatic group containing lubricant cinnamaldehyde, aromatic–aromatic as well as aromatic–aliphatic intermolecular interactions may be contributing towards slippery surface formation, Table 1.

Out of the three fluorinated pulsed plasma polymer coatings investigated for omniphobicity (poly(perfluoroallylbenzene), poly(pentafluorostyrene), and poly(1H, 1H, 2H, 2H-perfluorooctyl acrylate)), only the first one yielded a slippery surface when combined with fluorinated lubricants. The latter two contain carbon-hydrogen and carbon-oxygen bonds which most likely act to hinder the compatibility of the fluorinated

lubricants with the pulsed plasma polymer host matrix; whereas perfluoroallylbenzene is fully fluorinated, meaning it has good compatibility with the perfluorotributylamine and perfluoropolyether lubricants—thereby highlighting the importance of the surface chemistry/energy matching with the lubricant. US Food and Drug Administration (FDA) approved perfluorodecalin lubricant also produced a slippery surface when combined with pulsed plasma poly(perfluoroallylbenzene), Table 1.<sup>[8]</sup> Such omniphobic slippery surfaces (low contact angle hysteresis / sliding angle towards both polar and non-polar liquids), offer potential for protection against chemical and biological warfare agents as well as bloodphobicity for healthcare applications.<sup>[8],[55],[63]</sup>

Pulsed plasma poly(vinylpyridine) failed to form a slippery lubricant-infused surface when treated with lubricants, Supporting Information Table S 3. Pyridine is a relatively strong basic compound, with a  $pK_a$  value of 5.2, and can lead to hydrogen-bond formation (due to the nitrogen lone-pair electrons, which are orthogonal to the aromatic  $\pi$  orbitals, and therefore do not donate any electron density into aromatic  $\pi$  orbitals orbitals).<sup>[64]</sup> Indeed, pulsed plasma poly(vinylpyridine) has previously been described as 'superhydrophilic' and displays preferential wetting by water.<sup>[65]</sup> Furthermore, it has been reported that spin-coated poly(vinylpyridine) did not form a slippery surface with silicone oil lubricant due to preferential wetting by water.<sup>[66]</sup> In contrast, the aromatic pulsed plasma poly(vinylaniline), which contains a relatively polar amine group, has been shown in the present study to successfully form slippery surfaces, Table 1. The reason is that the nitrogen lone pair in the aniline ring is able to delocalise via resonance into the aromatic  $\pi$  system, giving rise to lower  $pK_a$  value of only 4.6, and the amine group does not form hydrogen bonds with water as readily compared to the pulsed plasma poly(vinylpyridine) system.<sup>[65]</sup> This manifests in the relatively higher static water contact angle for pulsed plasma poly(vinylaniline) versus pulsed plasma poly(vinylpyridine) ( $75^\circ$  and  $38^\circ$  respectively, Table 1 and Supporting Information Table S 3). Similarly, glycidyl methacrylate contains a polar epoxide group, and pulsed plasma poly(glycidyl methacrylate) exhibits a fairly low static water contact angle (i.e. it is hydrophilic), and thus does not form a slippery lubricant-infused coating, Supporting information Table S 4.

## 4. CONCLUSIONS

A range of slippery surfaces have been devised by combining different functional pulsed plasma polymer layers and lubricants to provide a molecular level structure–behaviour relationship. The fabrication process involves a simple, quick, substrate-independent, and conformal two-step methodology. Hydrophilic pulsed plasma polymer coatings are found not to produce slippery lubricant-infused coatings. Whilst the structure–behaviour relationship demonstrates that aromatic–aliphatic intermolecular interactions between coating and lubricant favours slippery surface formation. Fluorinated lubricant-infused coatings display omniphobicity and repel liquids with a range of surface tensions (including water, heptane and motor oil). Natural antimicrobial compound cinnamaldehyde-infused pulsed plasma polymer surfaces give rise to multifunctionality comprising liquid repellency (self cleaning) and antibacterial activity against both Gram-positive *Staphylococcus aureus* and Gram-negative *Escherichia coli*. In addition, these antimicrobial natural compound lubricant-infused pulsed plasma polymer surfaces repel a range of everyday liquid foodstuffs (such as tomato ketchup and honey). The successful production of slippery lubricant-infused surfaces on drop-cast polystyrene and pre-formed polystyrene plastic (from Petri dishes) demonstrates that this aromatic–aliphatic intermolecular interactions approach is not only limited to plasma polymer coatings, but potentially applicable to a range of alternative surface functionalisation methods including: atomised spray plasma deposition, initiated chemical vapour deposition, electron/ion beam deposition, self-assembled layers, as well as other dry and wet surface coating methods.

## 5. EXPERIMENTAL SECTION

### 5.1 Pulsed Plasmachemical Deposition

A cylindrical glass reactor (5.5 cm diameter, 475 cm<sup>3</sup> volume) housed within a Faraday cage was used for plasmachemical deposition. This was connected to a 30 L min<sup>-1</sup> rotary pump (model E2M2, Edwards Vacuum Ltd.) via a liquid nitrogen cold trap (base pressure less than  $2 \times 10^{-3}$  mbar and air leak rate better than  $6 \times 10^{-9}$  mol s<sup>-1</sup>). A copper coil wound around the reactor (4 mm diameter, 10 turns, located 10 cm downstream from the gas inlet) was connected to a 13.56 MHz radio frequency (RF)

power supply via an L–C matching network. A pulse signal generator was used to trigger the RF power supply. Prior to film deposition, the whole apparatus was thoroughly scrubbed using detergent and hot water, rinsed with propan-2-ol (+99.5 wt.%, Fisher Scientific UK Ltd.), oven dried at 150°C, and further cleaned using a 50 W continuous wave air plasma at 0.2 mbar for 30 min. Polyethylene terephthalate film (PET, capacitor grade, 0.10 mm thickness, Lawson Mardon Ltd.) or non-woven porous polypropylene cloth (0.41 mm thick,  $22.7 \pm 4.4 \mu\text{m}$  fibre diameter, with dimpled structure  $0.68 \pm 0.16 \text{ mm}$  separation, spunbond,  $70 \text{ g m}^{-2}$ , Avoca Technical Ltd.) was rinsed in absolute ethanol (+99.5 %, Fisher Scientific UK Ltd.) for 15 min prior to insertion into the centre of the plasma chamber. Silicon wafer (Silicon Valley Microelectronics Inc., orientation: <100>, resistivity: 5-20  $\Omega\cdot\text{cm}$ , thickness:  $525 \pm 25 \mu\text{m}$ , front surface: polished, back surface: etched) cleaning comprised sonication in a 50:50 100 ml mixture of propan-2-ol and cyclohexane (+99.7 wt.%, Sigma-Aldrich Ltd.) for 15 min prior to air drying and placement into the centre of the chamber. Further cleaning entailed running a 50 W continuous wave air plasma at 0.2 mbar for 30 min. The monomer precursor was loaded into a sealable glass tube, degassed via several freeze–pump–thaw cycles, and then attached to the reactor. Monomer vapour was then allowed to purge the apparatus at a pressure of typically 0.15–0.20 mbar (except benzyl acrylate, which had a vapour pressure of 0.08 mbar) for 15 min prior to electrical discharge ignition. An initial continuous wave plasma was run for 30 s to ensure good adhesion to the substrate before switching to pulsed mode required for well-defined plasmachemical deposition over a period lasting 30 min. Upon electrical discharge extinction, the precursor vapour was allowed to continue to pass through the system for a further 15 min, and then the chamber was evacuated to base pressure followed by venting to atmosphere.

Monomers utilised for pulsed plasmachemical deposition were: hexyl acrylate (98%, Sigma-Aldrich Ltd.), styrene (+99%, Sigma-Aldrich Ltd.), benzyl acrylate (+97%, Alfa Aesar, Fisher Scientific UK Ltd.), 3-vinylbenzaldehyde (+97%, Sigma-Aldrich Ltd.), vinylbenzyl chloride (+97%, mixture of 2-, 3- and 4- isomers, Sigma-Aldrich Ltd.), perfluoroallylbenzene (Fluorochem Ltd.), 4-vinylaniline (+97%, Fluorochem Ltd.), 4-vinylpyridine (+95%, Sigma-Aldrich Ltd.), glycidyl methacrylate (+97%, Sigma-Aldrich Ltd), pentafluorostyrene (Apollo Scientific Ltd.), and 1H, 1H, 2H, 2H-perfluorooctyl acrylate (+95%, Fluorochem Ltd.). The pulsed plasma deposition duty cycle parameters for each precursor are given in Supporting Information Table S 2. Less

than 0.1 ml of monomer was consumed during a typical pulsed plasma deposition experiment, which meant that there was negligible chemical waste.

## **5.2 Polystyrene Surfaces**

Polystyrene (pellets, average  $M_w$  280,000, Sigma-Aldrich Ltd.) was dissolved in chloroform (99.8+ %, Fisher Scientific UK Ltd.) to give a 5% w/v solution. Glass slides (15 mm x 15 mm) were cleaned ultrasonically in 100 ml of a 50:50 mixture of propan-2-ol and cyclohexane for 15 min and then dried. Several drops of the polystyrene solution were placed onto the glass slide so that the entire surface was covered. The solvent was allowed to evaporate under ambient conditions at 20°C. In addition, polystyrene petri dishes (Fisherbrand™ polystyrene Petri dishes, Fisher Scientific UK Ltd.) were cut into small pieces (15 mm x 15 mm).

## **5.3 Formation of Slippery Lubricant-Infused Surfaces**

The lubricants used were: cinnamaldehyde (99%, Acros Organics brand, Fisher Scientific UK Ltd.), citral (95%, mixture of isomers, Acros Organics brand, Fisher Scientific UK Ltd.), decanal (>98%, Mystic Moments Madar Corporation Ltd.), 2-methylundecanal (>98%, Mystic Moments Madar Corporation Ltd.), hexadecane (99%, Sigma-Aldrich Ltd.), perfluorodecalin (90%, mixture of cis and trans isomers, Acros Organics brand, Fisher Scientific UK Ltd.), perfluorotributylamine (Fluorinert FC-43, 3M Inc.), and perfluoropolyether (Fomblin® Y LVAC 06/6, Ausimont Ltd.).

Lubricant infused surfaces were prepared by immersing the coated substrate into several millilitres of the neat lubricant liquid at 20°C for 15 min. Afterwards, the substrates were removed from solution, placed in deionised water and shaken for 5 min, followed by removal and drying in air for at least 3 h at 20°C, with the samples stood upright to allow any excess lubricant to run off directly onto tissue paper—the quantities of lubricant were very small, and the tissue paper was subsequently placed into the appropriate laboratory chemical waste category, for safe disposal in a controlled manner.

Control substrates were prepared by immersing untreated PET film substrates into the lubricant and removing any excess lubricant as described above.

## 5.4 Coating Characterisation

Infrared spectra were acquired using a FTIR spectrometer equipped with a liquid nitrogen cooled MCT detector (model Spectrum One, PerkinElmer Inc.). Spectra were collected at  $4\text{ cm}^{-1}$  resolution across the  $400\text{--}4000\text{ cm}^{-1}$  range and averaged over 100 scans. Attenuated total reflectance (ATR) infrared spectra were obtained using a diamond ATR accessory (model Golden Gate, Graseby Specac Ltd.). Reflection–absorption (RAIRS) measurements utilized a variable angle accessory (Graseby Specac Ltd.) fitted with a KRS-5 polarizer (to remove the s-polarized component) set at either  $55^\circ$  or  $66^\circ$  with respect to the surface normal.

Coating thicknesses were measured using a spectrophotometer (model nkd-6000, Aquila Instruments Ltd.), Supporting Information Table S 2. This entailed acquisition of transmittance–reflectance curves ( $350\text{--}1000\text{ nm}$  wavelength range) for each coated sample and fitting to a Cauchy model for dielectric materials using a modified Levenberg–Marquardt algorithm.

Atomic force microscopy (AFM) images were acquired using a Bruker MM8 Multimode AFM scanning probe microscope. Scans were made with at least 256 line resolution in Peakforce QNM mode at  $1\text{ kHz}$  in the vertical direction, and Nunano Scout 150 probes with a nominal force constant of  $18\text{ N m}^{-1}$ . Images were analysed using Gwyddion v2.53 software. Root-mean-square roughness values ( $Roughness_{\text{RMS}}$ ) were calculated over  $1\text{ }\mu\text{m} \times 1\text{ }\mu\text{m}$  scan areas.

## 5.5 Contact Angle Analysis

Sessile drop static contact angle measurements were carried out at  $20^\circ\text{C}$  using a video capture apparatus in combination with a motorised syringe (model VCA 2500XE, A.S.T. Products Inc.).  $2.0\text{ }\mu\text{l}$  droplets of ultrapure water were employed to assess hydrophobicity. Advancing and receding contact angle values were determined by respectively increasing the dispensed  $2.0\text{ }\mu\text{l}$  liquid drop volume by a further  $2.0\text{ }\mu\text{l}$  at a rate of  $0.1\text{ }\mu\text{l s}^{-1}$ , and then decreasing the liquid drop volume at a rate of  $0.1\text{ }\mu\text{l s}^{-1}$ .<sup>[67]</sup> Measurements were repeated at least 3 times.

## 5.6 Sliding Angle Analysis

Sliding angle measurements were carried out at 20°C using a V-block adjustable angle gauge (model Adjustable Angle Gauge/Tilting Vee Blocks small, Arc Euro Trade Ltd.). Samples were placed onto the stage with an initial angle of 0°. A 50 µl droplet of deionised water was dispensed onto the sample, and the tilt angle was slowly increased at a rate of 1° every 5 s until movement of the water droplet was observed.<sup>[68],[69]</sup> Measurements were repeated at least 3 times.

Heptane (99%, Sigma-Aldrich Inc.), motor engine oil (GTX Magnatec 15W-40, Castrol Ltd.), and vacuum pump oil (Ultragrade Performance 19 Vacuum Oil, Edwards Vacuum Ltd.) were tested for the poly(perfluoroallylbenzene)-perfluoropolyether coating in the same way.

For longevity and regeneration testing, slippery lubricant-infused surfaces were prepared on PET film pieces as previously described. Samples were subsequently left to sit under ambient conditions for a period of 4–5 months. Samples were then qualitatively assessed for slippery behaviour by placing drops of deionised water onto the samples—if the droplets were found to easily slide off at low tilt angles, the sample was considered to be still slippery, whereas if the droplets were seen not to move, to only slide at high tilt angles, or to wet the sample, then the sample was considered to have lost its slippery behaviour. Samples which had lost their slippery behaviour during storage were regenerated by immersion in a few millilitres of the relevant neat lubricant liquid for 5 min, washing in deionised water with shaking for 5 min, followed by removal and drying in air for at least 3 h at 20°C. Samples were then tested for slippery behaviour as described earlier.

## 5.7 Foodstuffs Repellency

Pulsed plasma poly(vinylaniline) was deposited onto the insides of glass vials. Slippery lubricant-infused surfaces were produced by filling these vials with either cinnamaldehyde, citral, decanal, or 2-methylundecanal. The vials were left to stand with the lids closed for 15 min. Next, the aldehyde liquid was discarded from the vials and the vials were upturned to dry with lids off for 15 min so that any excess unbound lubricant could run off. The vials were then rinsed twice with deionised water to help remove any remaining unbound lubricant, and subsequently upturned to dry for 15

min. Finally, the vials were turned upright and dried for a further 15 min before use. Uncoated glass vials were treated with aldehyde liquids in the same way to serve as controls.

Tomato ketchup and clear honey (Sainsbury's Supermarkets Ltd.) were used for repellency testing. Approximately a few millilitres of the foodstuff was dispensed into the glass vials. The vials were then upturned, and the behaviour of the foodstuffs recorded using a video camera.

## 5.8 Antibacterial Testing

Gram-negative *Escherichia coli* BW25113 (CGSC 7636; *rrnB3*  $\Delta$ *lacZ4787* *hsdR514*  $\Delta$ (*araBAD*)567  $\Delta$ (*rhaBAD*)568 *rph-1*) and Gram-positive *Staphylococcus aureus* (FDA209P, an MSSA strain; ATCC 6538P) bacterial cultures were prepared using autoclaved (Autoclave Vario 1528, Dixons Ltd.) Luria-Bertani broth media (LB; L3022, Sigma-Aldrich Ltd., 2% w/v in Milli-Q<sup>®</sup> grade water). A 5 ml bacterial culture was grown from a single colony for 16 h at 37°C, and then 50  $\mu$ L used to inoculate a sterile polystyrene cuvette (Catalogue No. 67.742, Sarstedt AG) containing 1 mL of LB Broth. The cuvette was covered with Parafilm (Cole-Parmer Ltd.) and then placed inside a shaking incubator (model Stuart Orbital Incubator S1500, Cole-Parmer Ltd.) set at 37°C and 120 rpm. An optical density  $OD_{600nm} = 0.4$  was verified using a UV-Vis spectrophotometer (model Jenway 6300, Cole-Parmer Ltd.) to obtain bacteria at the mid-log phase of growth.

Uncoated control samples were washed in absolute ethanol for 15 min and then dried under vacuum in order to make sure they were sterile and clean. Coated samples were sterile when taken out of the plasma deposition chamber due to the inherent sterilisation characteristics of electrical discharges which is attributed to their constituent electrons, ions, metastables, and vacuum-UV photons.<sup>[70]</sup> Sterile microtubes (1.5 mL, Sarstedt AG) were loaded with the untreated, or coated substrates. Next, 100  $\mu$ L of the prepared bacterial culture was pipetted onto each substrate placed aseptically inside a microtube so that the microorganisms could interact with one side of the surface. In practice, for non-porous substrates the liquid spread over the whole area of the sample. The microtube lid was closed, to prevent the sample drying out, and the tube placed horizontally on a sample tray and incubated (model Bacterial Incubator 250, LMS Ltd.) without shaking for 4 h at 30°C. Next, 900

$\mu\text{L}$  of autoclaved Luria-Bertani broth media was pipetted into each microtube and vortexed (model Vortex-Genie 2, Scientific Industries Inc.) in order to recover the bacteria as a 10-fold dilution ( $10^{-1}$ ). Further ten-fold serial dilutions were undertaken to provide  $10^{-2}$ ,  $10^{-3}$ ,  $10^{-4}$ ,  $10^{-5}$  and  $10^{-6}$  samples. Colony-forming unit (CFU) plate counting was performed by placing 10  $\mu\text{L}$  drops from each diluted sample ( $10^{-1}$  to  $10^{-6}$  dilutions) onto autoclaved Luria-Bertani Agar solid plates (EZMix™ powder, dust free, fast dissolving fermentation medium, L7533, Sigma-Aldrich Ltd.) and incubated (model Bacterial Incubator 250, LMS Ltd.) for 16 h at 30°C. The number of colonies visible at each dilution were then counted. All tests were performed in triplicate. The  $\text{Log}_{10}$  Reduction value for a treated sample was calculated relative to a control untreated sample. For each experiment, treated and untreated substrates were exposed to bacteria in parallel and incubated under identical conditions for the same time period before recovery and viability measurement. This test method to quantify the number of bacteria killed following exposure to treated substrates was chosen because cinnamaldehyde is not readily soluble in aqueous media and therefore its efficacy will be localised at the functionalised substrate surface which promotes compatibility with cinnamaldehyde. The high numbers of bacteria recovered from untreated substrates provides good evidence that the method is effective. Furthermore, the vortex mixer agitates the samples at 2000–3000 rpm and is fully capable of removing bacteria from surfaces.<sup>[71]</sup>

For antibacterial recycling tests the same procedure as described above was followed, with the variation that, following 4 h incubation, the substrates were taken out from the  $10^{-1}$  dilution solution microtubes, rinsed with ultrapure water (approximately 50 ml) for 1 min at 20°C and then completely air-dried overnight before the next use. Consecutive repeat tests were performed using the same samples, with the mid-log bacterial culture being placed on the same side of the substrate each time. All tests were performed in triplicate.

## **6. SUPPORTING INFORMATION**

Coating thickness values, water droplet contact angle values, water droplet sliding angle values, infrared spectra, antibacterial test  $\text{Log}_{10}$  Reduction values, and liquid repellency videos are provided as Supporting Information.

## 7. ACKNOWLEDGEMENTS

J. P. S. B. and H. J. C. devised the concept. H. J. C. performed sample preparation, water contact angle and sliding angle measurements, infrared spectroscopy, and food repellency tests. C. P. G. acquired atomic force microscopy images. H. J. C. and G. J. S. carried out antibacterial testing. J. P. S. B. and H. J. C. jointly drafted the manuscript. All authors gave final approval for publication. This work was financially supported by the British Council (Katip Çelebi – Newton Fund grant reference 333595).

## 8. CONFLICT OF INTEREST

Durham University has filed an international patent application.

## 9. DATA AVAILABILITY

Data created during this research can be accessed at <https://collections.durham.ac.uk>

## 10. REFERENCES

- [1] U. Bauer, W. Federle, *Plant Signal. Behav.* **2009**, *4*, 1019.
- [2] H.F. Bohn, W. Federle, *Proc. Natl. Acad. Sci. U. S. A.* **2004**, *101*, 14138.
- [3] V. B. Wright, W. K. Poulson, W. M. Mackintosh, G.B. 190325000A, **1904**.
- [4] J. A. Vielle, G.B. 209138A, **1924**.
- [5] T.S. Wong, S.H. Kang, S.K.Y. Tang, E.J. Smythe, B.D. Hatton, A. Grinthal, J. Aizenberg, *Nature* **2011**, *477*, 443.
- [6] A.K. Epstein, T.S. Wong, R.A. Belisle, E.M. Boggs, J. Aizenberg, *Proc. Natl. Acad. Sci. U. S. A.* **2012**, *109*, 13182.
- [7] L. Xiao, J. Li, S. Mieszkin, A. Di Fino, A.S. Clare, M.E. Callow, J.A. Callow, M. Grunze, A. Rosenhahn, P.A. Levkin, *ACS Appl. Mater. Interfaces* **2013**, *5*, 10074.
- [8] D.C. Leslie, A. Waterhouse, J.B. Berthet, T.M. Valentin, A.L. Watters, A. Jain, P. Kim, B.D. Hatton, A. Nedder, K. Donovan, E.H. Super, C. Howell, C.P. Johnson, T.L. Vu, D.E.

- Bolgen, S. Rifai, A.R. Hansen, M. Aizenberg, M. Super, J. Aizenberg, D.E. Ingber, *Nat. Biotechnol.* **2014**, *32*, 1134.
- [9] S. Ozbay, C. Yuceel, H.Y. Erbil, *ACS Appl. Mater. Interfaces* **2015**, *7*, 22067.
- [10] J. Zhang, C. Gu, J. Tu, *ACS Appl. Mater. Interfaces* **2017**, *9*, 11247.
- [11] T.V.J. Charpentier, A. Neville, S. Baudin, M.J. Smith, M. Euvrard, A. Bell, C. Wang, R. Barker, *J. Colloid Interface Sci.* **2015**, *444*, 81.
- [12] B.L. Wang, L. Heng, L. Jiang, *ACS Appl. Mater. Interfaces* **2018**, *10*, 7442.
- [13] H. Luo, Y. Lu, S. Yin, S. Huang, J. Song, F. Chen, F. Chen, C.J. Carmalt, I.P. Parkin, *J. Mater. Chem. A* **2018**, *6*, 5635.
- [14] X. Dai, N. Sun, S.O. Nielsen, B.B. Stogin, J. Wang, S. Yang, T.S. Wong, *Sci. Adv.* **2018**, *4*, eaaq0919.
- [15] Q. Li, Z. Guo, *J. Colloid Interface Sci.* **2019**, *536*, 507.
- [16] R. Mukherjee, M. Habibi, Z.T. Rashed, O. Berbert, X. Shi, J.B. Boreyko, *Sci. Rep.* **2018**, *8*, 1.
- [17] J. Wang, L. Wang, N. Sun, R. Tierney, H. Li, M. Corsetti, L. Williams, P.K. Wong, T.S. Wong, *Nat. Sustain.* **2019**, *2*, 1097.
- [18] J. Zhang, P. Liu, B. Yi, Z. Wang, X. Huang, L. Jiang, X. Yao, *ACS Nano* **2019**, *13*, 10596.
- [19] Y. Wang, H. Zhang, X. Liu, Z. Zhou, *J. Mater. Chem. A* **2016**, *4*, 2524.
- [20] D.R.M. Smith, K.B. Pouwels, S. Hopkins, N.R. Naylor, T. Smieszek, J. V. Robotham, *J. Hosp. Infect.* **2019**, *103*, 44.
- [21] M.P. Schultz, J.A. Bendick, E.R. Holm, W.M. Hertel, *Biofouling* **2011**, *27*, 87.
- [22] E.A. Araújo, N.J. de Andrade, L.H.M. da Silva, A.F. de Carvalho, C.A.S. de Silva, A.M. Ramos, *Food Bioprocess Technol.* **2010**, *3*, 321.
- [23] S. Yuan, Z. Li, L. Song, H. Shi, S. Luan, J. Yin, *ACS Appl. Mater. Interfaces* **2016**, *8*, 21214.
- [24] U. Manna, N. Raman, M.A. Welsh, Y.M. Zayas-Gonzalez, H.E. Blackwell, S.P. Palecek, D.M. Lynn, *Adv. Funct. Mater.* **2016**, *26*, 3599.
- [25] J. Lee, J. Yoo, J. Kim, Y. Jang, K. Shin, E. Ha, S. Ryu, B.G. Kim, S. Wooh, K. Char, *ACS Appl. Mater. Interfaces* **2019**, *11*, 6550.
- [26] N. Tatarazako, H. Ishibashi, K. Teshima, K. Kishi, K. Arizono, *Environ. Sci.* **2004**, *11*, 133.
- [27] A. Panáček, L. Kvítek, M. Smékalová, R. Večeřová, M. Kolář, M. Röderová, F. Dyčka, M. Šebela, R. Pucek, O. Tomanec, R. Zbořil, *Nat. Nanotechnol.* **2018**, *13*, 65.
- [28] S. Yu, Y. Yin, J. Liu, *Environ. Sci. Process. Impacts* **2013**, *15*, 78.
- [29] A. Yan, Z. Chen, *Int. J. Mol. Sci.* **2019**, *20*, 1003.
- [30] Y. Tuo, H. Zhang, W. Chen, X. Liu, *Appl. Surf. Sci.* **2017**, *423*, 365.
- [31] P. Wang, D. Zhang, S. Sun, T. Li, Y. Sun, *ACS Appl. Mater. Interfaces* **2017**, *9*, 972.
- [32] T. Xiang, M. Zhang, H.R. Sadig, Z. Li, M. Zhang, C. Dong, L. Yang, W. Chan, C. Li, *Chem. Eng. J.* **2018**, *345*, 147.
- [33] H. Niemelä-Anttonen, H. Koivuluoto, M. Tuominen, H. Teisala, P. Juuti, J. Haapanen, J. Harra, C. Stenroos, J. Lahti, J. Kuusipalo, J.M. Mäkelä, P. Vuoristo, *Adv. Mater. Interfaces* **2018**, *5*, 1800828.
- [34] X. He, F. Tian, X. Bai, C. Yuan, *Colloids Surf. B Biointerfaces* **2019**, *184*, 110502.

- [35] M.E. Ryan, A.M. Hynes, J.P.S. Badyal, *Chem. Mater.* **1996**, *8*, 37.
- [36] A. Carletto, J.P.S. Badyal, *Phys. Chem. Chem. Phys.* **2019**, *21*, 16468.
- [37] T.A. Miller, M.G. Mikhael, R. Ellwanger, A. Boufelfel, D. Booth, A. Yializis, *MRS Proceedings* **1999**, *555*, 247.
- [38] G. Singh, S. Maurya, M.P. deLampasona, C.A.N. Catalan, *Food Chem. Toxicol.* **2007**, *45*, 1650.
- [39] S. Burt, *Int. J. Food Microbiol.* **2004**, *94*, 223.
- [40] K. Hayashi, N. Imanishi, Y. Kashiwayama, A. Kawano, K. Terasawa, Y. Shimada, H. Ochiai, *Antiviral Res.* **2007**, *74*, 1.
- [41] S. Shreaz, W.A. Wani, J.M. Behbehani, V. Raja, M. Irshad, M. Karched, I. Ali, W.A. Siddiqi, L.T. Hun, *Fitoterapia* **2016**, *112*, 116.
- [42] K. Fisher, C.A. Phillips, *J. Appl. Microbiol.* **2006**, *101*, 1232.
- [43] K. Liu, Q. Chen, Y. Liu, X. Zhou, X. Wang, *J. Food Sci.* **2012**, *77*, C1156.
- [44] I. Kubo, K.I. Fujita, A. Kubo, K.I. Nihei, T. Ogura, *J. Agric. Food Chem.* **2004**, *52*, 3329.
- [45] J.M. Al-Shuneigat, I.N. Al-Tarawneh, M.A. Al-Qudah, S.A. Al-Sarayreh, Y.M. Al-Saraireh, K.Y. Alsharafa, *Jordan J. Biol. Sci.* **2015**, *8*, 139.
- [46] Title 21–Food and Drugs; Chapter I–Food and Drug Administration; Department of Health and Human Services; Subchapter B–Food for Human Consumption (Continued); Part 182 Substances Generally Recognized as Safe. [https://www.accessdata.fda.gov/scripts/cdrh/cfdocs/cfcfr/cfrsearch.cfm?cfrpart=182&sho\\_wfr=1](https://www.accessdata.fda.gov/scripts/cdrh/cfdocs/cfcfr/cfrsearch.cfm?cfrpart=182&sho_wfr=1) Accessed Oct. **2021**.
- [47] Safety Evaluation of Certain Food Additives and Contaminants; WHO Food Additives Series 40. <http://www.inchem.org/documents/jecfa/jecmono/v040je11.htm> Accessed Oct. **2021**.
- [48] W.C.E. Schofield, J.P.S. Badyal, *Plasma Chem. Plasma Process.* **2006**, *26*, 361.
- [49] S.R. Coulson, I.S. Woodward, J.P.S. Badyal, S.A. Brewer, C. Willis, *Chem. Mater.* **2000**, *12*, 2031.
- [50] S. Morsch, W.C.E. Schofield, J.P.S. Badyal, *Langmuir* **2010**, *26*, 12342.
- [51] L. Wang, T.J. McCarthy, *Angew. Chemie - Int. Ed.* **2016**, *55*, 244.
- [52] J. Fang, Y. Xuan, Q. Li, *Sci. China Technol. Sci.* **2010**, *53*, 3088.
- [53] A. Hynes, J.P.S. Badyal, *Chem. Mater.* **1998**, *10*, 2177.
- [54] R. D. Chambers, *Fluorine in Organic Chemistry*; Wiley & Sons: London, **1973**.
- [55] N. Singh, H. Kakiuchida, T. Sato, R. Hönes, M. Yagihashi, C. Urata, A. Hozumi, *Langmuir* **2018**, *34*, 11405.
- [56] L.G. Harris, W.C.E. Schofield, K.J. Doores, B.G. Davis, J.P.S. Badyal, *J. Am. Chem. Soc.* **2009**, *131*, 7755.
- [57] J.T. Cohen, G. Carlson, G. Charnley, D. Coggon, E. Delzell, J.D. Graham, H. Greim, D. Krewski, M. Medinsky, R. Monson, D. Paustenbach, B. Petersen, S. Rappaport, L. Rhomberg, P. Barry Ryan, K. Thompson, *J. Toxicol. Environ. Heal. - Part B Crit. Rev.* **2002**, *5*, 1.
- [58] US Environmental Protection Agency Office, Protocol for the Evaluation of Bactericidal Activity of Hard, Non-porous Copper/Copper-Alloy Surfaces. **2015**.
- [59] C. Urata, G.J. Dunderdale, M.W. England, A. Hozumi, *J. Mater. Chem. A* **2015**, *3*, 12626.

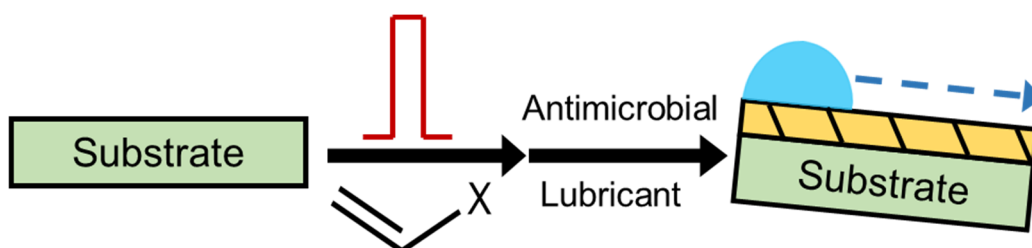
- [60] C. Howell, T.L. Vu, J.J. Lin, S. Kolle, N. Juthani, E. Watson, J.C. Weaver, J. Alvarenga, J. Aizenberg, *ACS Appl. Mater. Interfaces* **2014**, *6*, 13299.
- [61] D.B. Ninković, D.Z. Vojislavljević-Vasilev, V.B. Medaković, M.B. Hall, E.N. Brothers, S.D. Zarić, *Phys. Chem. Chem. Phys.* **2016**, *18*, 25791.
- [62] R. Togasawa, M. Tenjimbayashi, T. Matsubayashi, T. Moriya, K. Manabe, S. Shiratori, *ACS Appl. Mater. Interfaces* **2018**, *10*, 4198.
- [63] Q. Truong, Dual Hierarchical Omniphobic and Superomniphobic Coatings. U.S. 10253451, **2019**.
- [64] T.M. Krygowski, H. Szatyłowicz, J.E. Zachara, *J. Org. Chem.* **2005**, *70*, 8859.
- [65] R.P. Garrod, L.G. Harris, W.C.E. Schofield, J. McGettrick, L.J. Ward, D.O.H. Teare, J.P.S. Badyal, *Langmuir* **2007**, *23*, 689.
- [66] C.S. Ware, T. Smith-Palmer, S. Peppou-Chapman, L.R.J. Scarratt, E.M. Humphries, D. Balzer, C. Neto, *ACS Appl. Mater. Interfaces* **2018**, *10*, 4173.
- [67] R. E Johnson Jr, R. H. Dettre, in *Wettability*, (Ed: J. C. Berg), Marcel Dekker, Inc., New York, **1993**; Chapter 1, p 13.
- [68] E. Pierce, F.J. Carmona, A. Amirfazli, *Colloids Surfaces A Physicochem. Eng. Asp.* **2008**, *323*, 73.
- [69] C.C. Chang, C.J. Wu, Y.J. Sheng, H.K. Tsao, *RSC Adv.* **2016**, *6*, 19214.
- [70] M. Moisan, J. Barbeau, S. Moreau, J. Pelletier, M. Tabrizian, L. Yahia, *Int. J. Pharm.* **2001**, *226*, 1.
- [71] H.J. Cox, J. Li, P. Saini, J.R. Paterson, G.J. Sharples, J.P.S. Badyal, *J. Mater. Chem. B* **2021**, *9*, 2918.

## TABLE OF CONTENTS ENTRY

Structure–behaviour investigation shows that aromatic group containing nanocoatings infused with antimicrobial lubricants yield slippery bactericidal surfaces capable of repelling a wide range of liquids (including everyday foodstuffs such as tomato ketchup and honey). The slippery surface behaviour is attributed to aromatic–aliphatic intermolecular interactions.

*Harrison J. Cox, Colin P. Gibson, Gary J. Sharples, and Jas Pal S. Badyal\**

### Nature Inspired Substrate-Independent Omniphobic and Antimicrobial Slippery Surfaces



## **SUPPORTING INFORMATION**

### **Nature Inspired Substrate-Independent Omniphobic and Antimicrobial Slippery Surfaces**

*Harrison J. Cox, Colin P. Gibson, Gary J. Sharples, and Jas Pal S. Badyal\**

## 1. RESULTS

Table S 1. Water droplet static, advancing, receding, and hysteresis contact angle values and water droplet sliding angle values following lubricant treatment of uncoated PET film substrates. Values are reported as mean  $\pm$  standard deviation.

Surface	Contact Angle / °		Sliding Angle / °
	Static	Hysteresis	
PET	66.8 $\pm$ 1.6	52 $\pm$ 4	48 $\pm$ 2
PET–Cinnamaldehyde	71 $\pm$ 4	40 $\pm$ 4	27.3 $\pm$ 0.5
PET–Citral	64 $\pm$ 3	46 $\pm$ 4	29 $\pm$ 1
PET–Decanal	71.9 $\pm$ 1.6	29 $\pm$ 6	10.3 $\pm$ 0.5
PET– 2-Methylundecanal	65 $\pm$ 3	20 $\pm$ 1.5	10.0 $\pm$ 0.0
PET–Hexadecane	67 $\pm$ 4	20 $\pm$ 4	24.7 $\pm$ 1.7
PET–Perfluorotributylamine	114 $\pm$ 2	53 $\pm$ 3	29 $\pm$ 2
PET–Perfluoropolyether	82 $\pm$ 6	58 $\pm$ 8	41.0 $\pm$ 1.6
PET–Perfluorodecalin	100 $\pm$ 5	81 $\pm$ 5	57 $\pm$ 2

Table S 2. Pulsed plasma deposition parameters for deposited polymer coatings, film thicknesses values and deposition rates.

<b>Monomer</b>	<b>Peak Power / W</b>	<b><math>t_{on}</math> / <math>\mu</math>s</b>	<b><math>t_{off}</math> / ms</b>	<b>Deposition Temperature / °C</b>	<b>Film Thickness / nm</b>	<b>Deposition Rate / nm min<sup>-1</sup></b>
Hexyl acrylate	40	20	20	20	373	12.4
Styrene	30	100	4	20	200	6.7
Benzyl acrylate	40	20	20	20	168	5.6
3-Vinylbenzaldehyde	30	100	4	20	1242	41.4
Vinylbenzyl chloride	30	100	4	20	1774	59.1
Perfluoroallylbenzene	40	100	4	20	1363	45.4
4-Vinylaniline	40	100	4	40	177	5.9
4-Vinylpyridine	40	100	4	20	341	11.4
Glycidyl methacrylate	40	20	20	20	304	10.1
Pentafluorostyrene	30	100	4	20	1558	51.9
1H, 1H, 2H, 2H-Perfluorooctyl acrylate	40	20	20	20	1214	40.5

## 1.1 Pulsed Plasma Poly(Vinylpyridine)

Infrared spectroscopy of vinylpyridine monomer showed the following characteristic bands: C–H stretches ( $3100\text{--}2885\text{ cm}^{-1}$ ), ring summations ( $2000\text{--}1700\text{ cm}^{-1}$ ), vinyl C=C stretching ( $1633\text{ cm}^{-1}$ ), aromatic quadrant C=C stretching ( $1595\text{ cm}^{-1}$  and  $1547\text{ cm}^{-1}$ ), aromatic semicircle C=C and C=N stretching ( $1494\text{ cm}^{-1}$  and  $1408\text{ cm}^{-1}$  respectively), and vinyl =CH<sub>2</sub> wag ( $922\text{ cm}^{-1}$ ), Supporting Information Figure S 1.<sup>[1]</sup> Pulsed plasma deposited poly(vinylpyridine) showed good structural retention, with the disappearance of the vinyl group bands indicating that polymerisation had taken place.

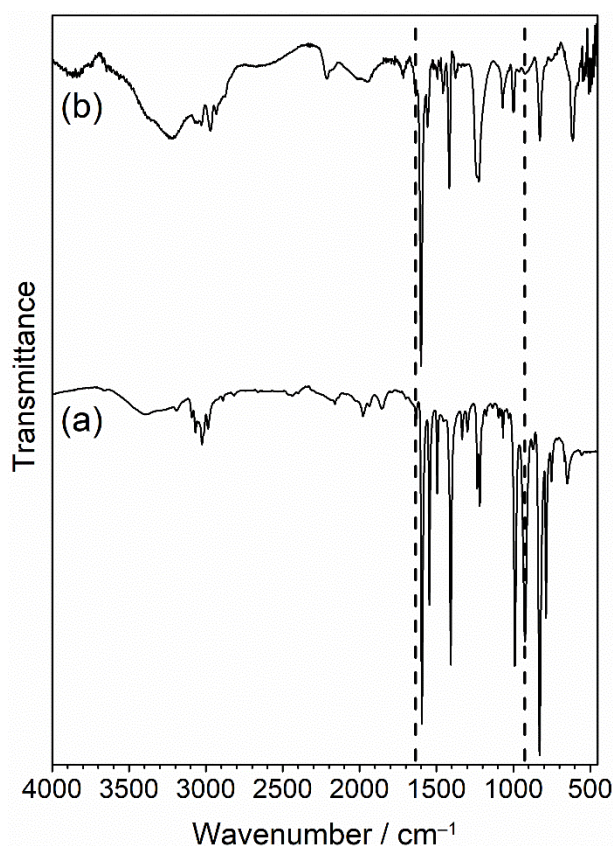


Figure S 1. Infrared spectra of: (a) vinylpyridine monomer (ATR); and (b) pulsed plasma poly(vinylpyridine) deposited onto silicon wafer (RAIRS, 55°). The dashed lines correspond to vinyl group absorbances ( $1633\text{ cm}^{-1}$  and  $922\text{ cm}^{-1}$ ).

Pulsed plasma poly(vinylpyridine)-only coatings were hydrophilic and showed water droplet pinning on the receding angles. Contact angle hysteresis for pulsed plasma poly(vinylpyridine) demonstrated that all the tested lubricants (cinnamaldehyde, decanal, 2-methylundecanal, and hexadecane) failed to infuse into

the poly(vinylpyridine) plasma polymer and produce slippery coatings, and also demonstrated that the poly(vinylpyridine) coating showed preferential wetting with water, Table S 3. Cinnamaldehyde caused at least partial washing off or dissolving of the coating, as determined by the loss of the brown colour of the coating (hence the lack of pinning on receding angles). Perfluorotributylamine failed to make the coating slippery, as seen from qualitative assessment of the sliding angle (quantitative analysis of contact angle hysteresis and sliding angle was not measured).

Table S 3. Water droplet static, advancing, receding, hysteresis contact angle values following lubricant impregnation of pulsed plasma poly(vinylpyridine)-coated PET film substrates. Values are reported as mean  $\pm$  standard deviation.

Surface	Contact Angle / °	
	Static	Hysteresis
PET	67 $\pm$ 2	52 $\pm$ 4
Pulsed Plasma Poly(vinylpyridine) (ppVP)	38 $\pm$ 5	57.4 $\pm$ 0.5
ppVP–Cinnamaldehyde	65 $\pm$ 9	38 $\pm$ 13
ppVP–Decanal	53 $\pm$ 5	69 $\pm$ 6
ppVP–2-Methylundecanal	49 $\pm$ 3	60 $\pm$ 3
ppVP–Hexadecane	43 $\pm$ 7	55 $\pm$ 10

## 1.2 Pulsed Plasma Poly(Glycidyl Methacrylate)

For glycidyl methacrylate monomer, the following characteristic infrared band assignments were as follows: epoxide ring C–H stretching ( $3062\text{ cm}^{-1}$ ), C–H stretching ( $3000\text{--}2880\text{ cm}^{-1}$ ), acrylate carbonyl C=O stretching ( $1714\text{ cm}^{-1}$ ), acrylate C=C stretching ( $1638\text{ cm}^{-1}$ ), epoxide ring breathing ( $1253\text{ cm}^{-1}$ ), antisymmetric epoxide ring deformation ( $908\text{ cm}^{-1}$ ), and symmetric epoxide ring deformation ( $842\text{ cm}^{-1}$ ), Supporting Information Figure S 2.<sup>[2]</sup> Loss of the acrylate carbon–carbon double bond after pulsed plasma deposition showed that polymerisation had successfully taken place. The epoxide bands are still visible, indicating good structural retention.

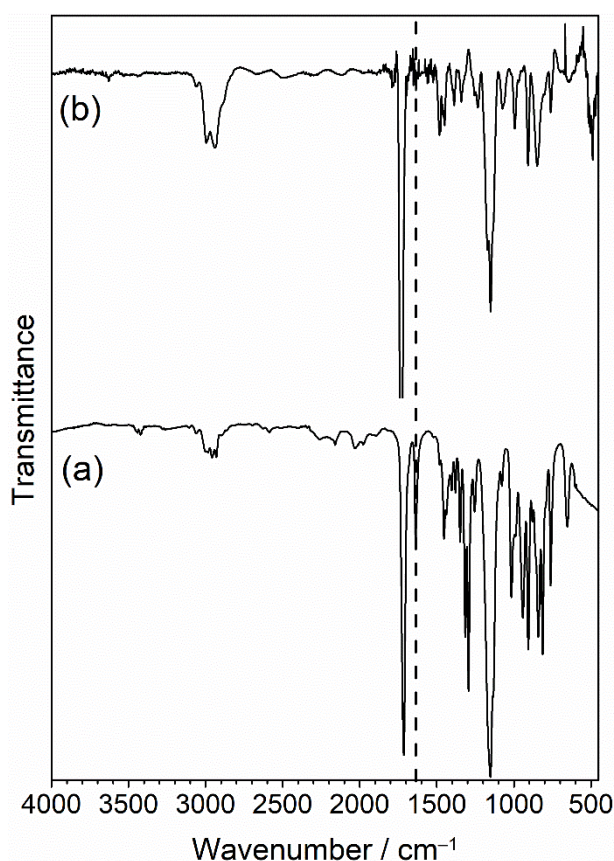


Figure S 2. Infrared spectra of: (a) glycidyl methacrylate monomer (ATR); and (b) pulsed plasma poly(glycidyl methacrylate) deposited onto silicon wafer (RAIRS,  $55^\circ$ ). The dashed line corresponds to acrylate carbon–carbon double bond absorbance ( $1638\text{ cm}^{-1}$ ).

None of the tested lubricants produced slippery surfaces with the pulsed plasma poly(glycidyl methacrylate) coating, Table S 4. In fact, they all resulted in an increase to the water contact angle hysteresis compared to the pulsed plasma

poly(glycidyl methacrylate)-only coating. Since the coatings were not slippery, sliding angles were not measured.

Table S 4. Water droplet static, advancing, receding, and hysteresis contact angle values following lubricant impregnation of pulsed plasma poly(glycidyl methacrylate)-coated PET film substrates. Values are reported as mean  $\pm$  standard deviation.

Surface	Contact Angle / °	
	Static	Hysteresis
PET	66.8 $\pm$ 1.6	52 $\pm$ 4
Pulsed Plasma Poly(GMA) (ppGMA)	56 $\pm$ 2	21.6 $\pm$ 0.8
ppGMA–Cinnamaldehyde	68 $\pm$ 2	35 $\pm$ 3
ppGMA–Decanal	68.1 $\pm$ 0.4	38 $\pm$ 4
ppGMA–2-Methylundecanal	57.0 $\pm$ 1.7	23 $\pm$ 4
ppGMA–Hexadecane	75.1 $\pm$ 0.7	42 $\pm$ 5

### 1.3 Pulsed Plasma Poly(Pentafluorostyrene)

Pentafluorostyrene monomer infrared spectra showed the following characteristic bands: vinyl C=C stretch ( $1625\text{ cm}^{-1}$ ), fluorinated aromatic ring vibrations ( $1519\text{ cm}^{-1}$  and  $1492\text{ cm}^{-1}$ ), C-F (aromatic) stretching ( $973\text{ cm}^{-1}$ ), and vinyl =CH<sub>2</sub> wag ( $927\text{ cm}^{-1}$ ), Supporting Information Figure S 3.<sup>[3]</sup> Disappearance of the vinyl group bands in the pulsed plasma deposited poly(pentafluorostyrene) showed that polymerisation had successfully taken place.

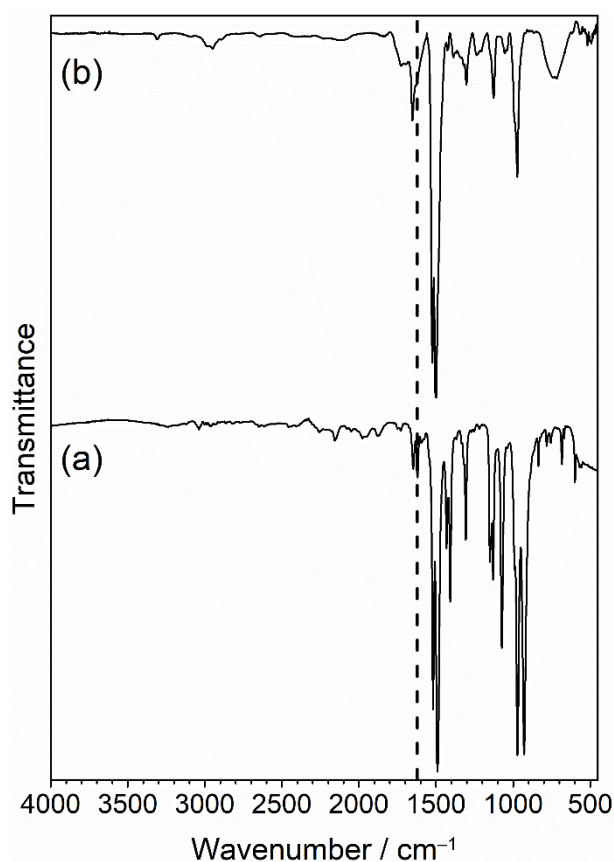


Figure S 3. Infrared spectra of: (a) pentafluorostyrene monomer (ATR); and (b) pulsed plasma poly(pentafluorostyrene) deposited onto silicon wafer (RAIRS, 55°). The dashed line corresponds to vinyl carbon-carbon double bond absorbance ( $1625\text{ cm}^{-1}$ ).

Pulsed plasma poly(pentafluorostyrene) coated PET substrates were treated with fluorinated lubricants (perfluorotributylamine and perfluoropolyether), but it was found that they did not produce slippery surfaces, and in fact the lubricants appeared to increase the water contact angle hysteresis compared to the pulsed plasma poly(pentafluorostyrene)-only coating, Table S 5. Since the coatings were not slippery, sliding angles were not measured.

Table S 5. Water droplet static, advancing, receding, and hysteresis contact angle values following lubricant impregnation of pulsed plasma poly(pentafluorostyrene)-coated PET film substrates. Values are reported as mean  $\pm$  standard deviation.

Surface	Contact Angle / °	
	Static	Hysteresis
PET	66.8 $\pm$ 1.6	52 $\pm$ 4
Pulsed Plasma Poly(pentafluorostyrene) (ppPFS)	96 $\pm$ 3	29.1 $\pm$ 1.4
ppPFS–Perfluorotributylamine	116.7 $\pm$ 0.5	43 $\pm$ 7
ppPFS–Perfluoropolyether	113.8 $\pm$ 1.3	30 $\pm$ 2

#### 1.4 Pulsed Plasma Poly(1H, 1H, 2H, 2H-Perfluorooctyl Acrylate)

1H, 1H, 2H, 2H-perfluorooctyl acrylate monomer infrared characteristic peaks were observed as follows: C–H stretching ( $2975\text{ cm}^{-1}$ ), acrylate carbonyl C=O stretch ( $1732\text{ cm}^{-1}$ ), C=C stretching ( $1638\text{ cm}^{-1}$ ), and C-F stretching ( $1260\text{--}1100\text{ cm}^{-1}$ ), Supporting Information Figure S 4.<sup>[4]</sup> The carbon–carbon double bond bands disappeared upon plasma polymerisation, indicating that polymerisation was successful.

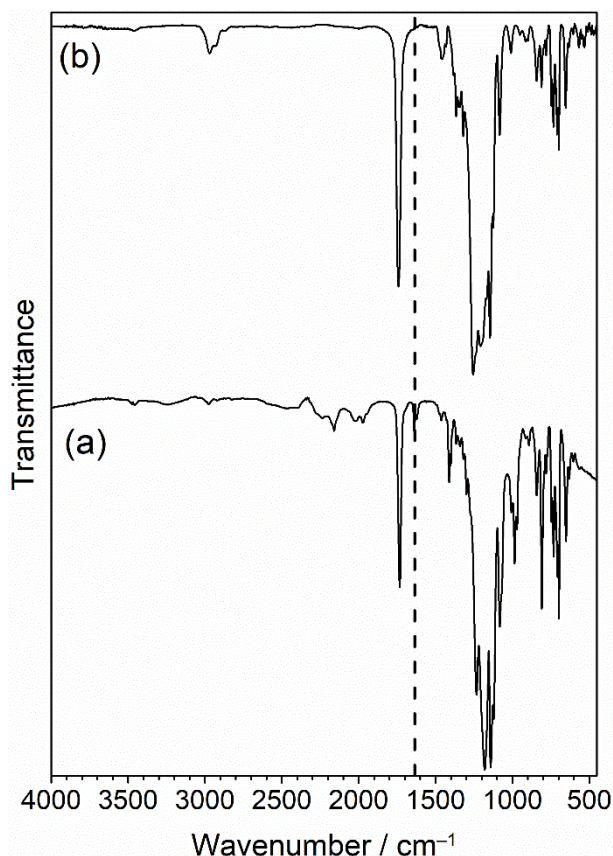


Figure S 4. Infrared spectra of: (a) 1H, 1H, 2H, 2H-perfluorooctyl acrylate monomer (ATR); and (b) pulsed plasma poly(1H, 1H, 2H, 2H-perfluorooctyl acrylate) deposited onto silicon wafer (RAIRS,  $55^\circ$ ). The dashed line corresponds to acrylate carbon–carbon double bond absorbance ( $1638\text{ cm}^{-1}$ ).

None of the pulsed plasma poly(1H, 1H, 2H, 2H-perfluorooctyl acrylate) coated samples produced slippery surfaces when immersed into either of the fluorinated lubricants, Table S 6. Perfluoropolyether did reduce the water contact angle hysteresis somewhat compared to the poly(1H, 1H, 2H, 2H-perfluorooctyl acrylate)-only coated surface, but the hysteresis was still relatively high. Since the coatings were not slippery, sliding angles were not measured.

Table S 6. Water droplet static, advancing, receding, and hysteresis contact angle values following lubricant impregnation of pulsed plasma poly(1H, 1H, 2H, 2H-perfluorooctyl acrylate)-coated PET film substrates. Values are reported as mean  $\pm$  standard deviation.

Surface	Contact Angle / °	
	Static	Hysteresis
PET	66.8 $\pm$ 1.6	52 $\pm$ 4
Pulsed Plasma 1H, 1H, 2H, 2H-perfluorooctyl acrylate (ppPFAC6)	122 $\pm$ 3	79 $\pm$ 9
ppPFAC6–Perfluorotributylamine	121.7 $\pm$ 0.3	72 $\pm$ 3
ppPFAC6–Perfluoropolyether	117 $\pm$ 3	33 $\pm$ 5

## 1.5 Pulsed Plasma Poly(Hexyl Acrylate)

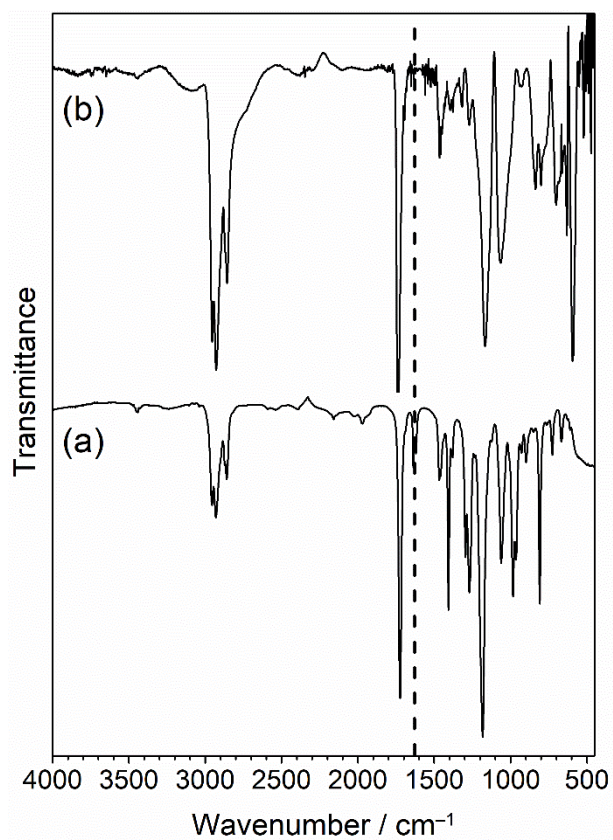


Figure S 5: Infrared spectra of: (a) hexyl acrylate monomer (ATR); and (b) pulsed plasma poly(hexyl acrylate) deposited onto silicon wafer (RAIRS, 55°). The dashed line corresponds to acrylate carbon-carbon double bond absorbance (1638 cm<sup>-1</sup>).

Table S 7. Water droplet static, advancing, receding, and hysteresis contact angle values following lubricant impregnation of pulsed plasma poly(hexyl acrylate) (ppHA) coated PET film substrates. Values are reported as mean  $\pm$  standard deviation.

Surface	Contact Angle / °	
	Static	Hysteresis
PET	66.8 $\pm$ 1.6	52 $\pm$ 4
Pulsed Plasma Poly(hexyl acrylate) (ppHA)	82.2 $\pm$ 0.8	8.5 $\pm$ 1.1
ppHA–Decanal	83 $\pm$ 5	8 $\pm$ 5
ppHA–Hexadecane	91.6 $\pm$ 1.0	11.4 $\pm$ 1.5
ppHA–2-Methylundecanal	73.8 $\pm$ 0.5	5.9 $\pm$ 1.5
ppHA–Cinnamaldehyde	71 $\pm$ 5	17 $\pm$ 9
ppHA–Perfluorotributylamine	83 $\pm$ 3	13 $\pm$ 6

## 1.6 Pulsed Plasma Poly(Styrene)

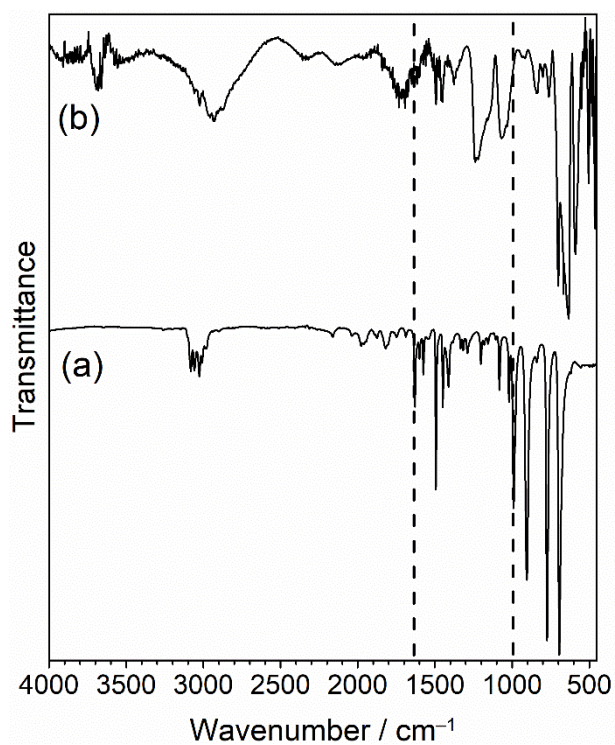


Figure S 6: Infrared spectra of: (a) styrene monomer (ATR); and (b) pulsed plasma poly(styrene) deposited onto silicon wafer (RAIRS,  $66^\circ$ ). The dashed lines correspond to vinyl group absorbances ( $1629 \text{ cm}^{-1}$  and  $994 \text{ cm}^{-1}$ ).

## 1.7 Pulsed Plasma Poly(Benzyl Acrylate)

Benzyl acrylate monomer displays the following characteristic infrared absorption bands: C–H stretching ( $3100\text{--}2850\text{ cm}^{-1}$ ), aromatic ring summations ( $2000\text{--}1800\text{ cm}^{-1}$ ), acrylate carbonyl C=O stretching ( $1720\text{ cm}^{-1}$ ), acrylate C=C stretching ( $1633\text{ cm}^{-1}$  and  $1621\text{ cm}^{-1}$ ), and the C–O ester stretch ( $1171\text{ cm}^{-1}$ ), Supporting Information Figure S 7. Similar to the alkyl acrylates, pulsed plasma deposited poly(benzyl acrylate) showed absence of the acrylate carbon–carbon double bond band, indicating that polymerisation had taken place, whereas the phenyl rings remain intact.

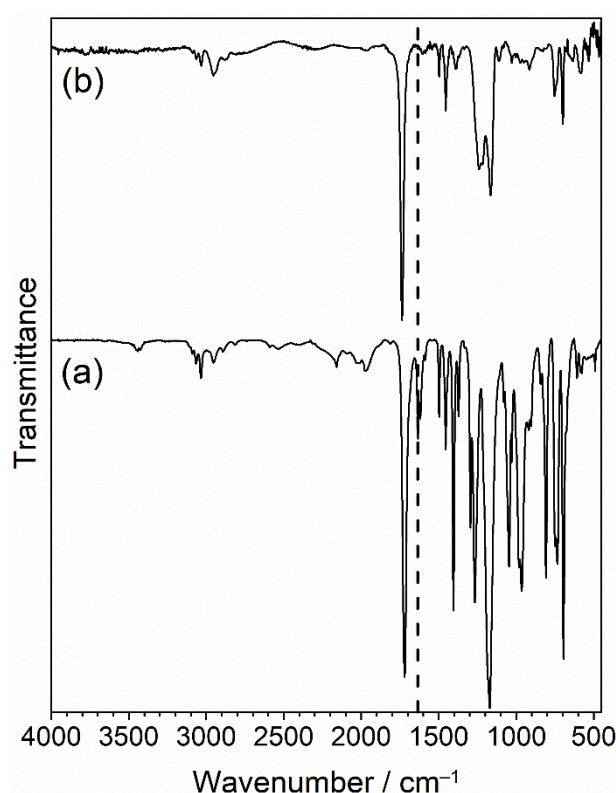


Figure S 7. Infrared spectra of: (a) benzyl acrylate monomer (ATR); and (b) pulsed plasma poly(benzyl acrylate) deposited onto silicon wafer (RAIRS,  $66^\circ$ ). The dashed line corresponds to acrylate carbon–carbon double bond absorbance ( $1633\text{ cm}^{-1}$ ).

Pulsed plasma polymerised poly(benzyl acrylate) showed large water contact angle hysteresis and sliding angle values, Table 1. Hexadecane-infused pulsed plasma poly(benzyl acrylate) coating gave rise to lower hysteresis and sliding angles, although not particularly low. Cinnamaldehyde-, decanal-, and 2-methylundecanal-infused pulsed plasma poly(benzyl acrylate) coatings all displayed water contact angle hysteresis and sliding angles  $< 5^\circ$ . In particular, the 2-methylundecanal-infused

coating showed excellent slippery properties, with a mean hysteresis of  $0.5^\circ$ , and a sliding angle of  $2^\circ$ .

## 1.8 Pulsed Plasma Poly(Vinylbenzaldehyde)

Vinylbenzaldehyde monomer displays the following characteristic infrared bands: C–H stretches ( $3090\text{--}2900\text{ cm}^{-1}$ ), aldehyde CHO stretches ( $2815\text{ cm}^{-1}$  and  $2726\text{ cm}^{-1}$ ), aldehyde C=O stretch ( $1695\text{ cm}^{-1}$ ), vinyl C=C stretch ( $1630\text{ cm}^{-1}$ ), di-substituted benzene quadrant stretch ( $1599\text{ cm}^{-1}$  and  $1582\text{ cm}^{-1}$ ), meta-substituted benzene semicircle stretch ( $1478\text{ cm}^{-1}$  and  $1445\text{ cm}^{-1}$ ), aldehyde CH rock ( $1378\text{ cm}^{-1}$ ), meta ring stretch ( $1143\text{ cm}^{-1}$ ), meta in-phase CH wag ( $990\text{ cm}^{-1}$ ), and meta single CH wag ( $908\text{ cm}^{-1}$ ), Supporting Information Figure S 8.<sup>[5]</sup>

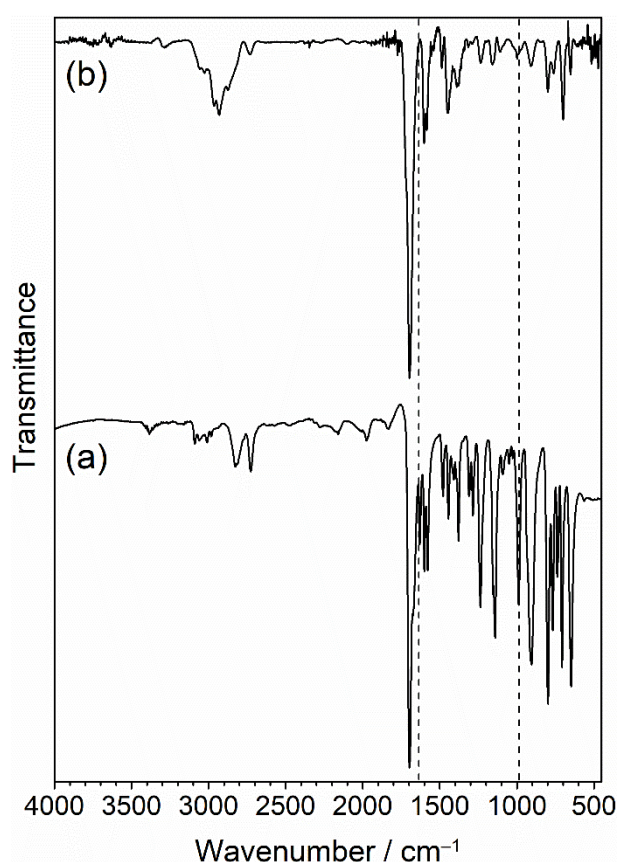


Figure S 8. Infrared spectra of: (a) vinylbenzaldehyde monomer (ATR); and (b) pulsed plasma poly(vinylbenzaldehyde) deposited onto silicon wafer (RAIRS,  $55^\circ$ ). The dashed lines correspond to vinyl group absorbances ( $1630\text{ cm}^{-1}$ ).

Pulsed plasma deposited poly(vinylbenzaldehyde) shows good structural retention and minimal cross-linking, as indicated by the retention of the aldehyde CHO stretches ( $2815\text{ cm}^{-1}$  and  $2726\text{ cm}^{-1}$ ), aldehyde C=O stretch ( $1695\text{ cm}^{-1}$ ), meta-substituted aromatic ring semicircle stretch ( $1478\text{ cm}^{-1}$  and  $1445\text{ cm}^{-1}$ ), and meta-substituted benzene semicircle stretch ( $1478\text{ cm}^{-1}$  and  $1445\text{ cm}^{-1}$ ). Disappearance of

the vinyl C=C stretch ( $1630\text{ cm}^{-1}$ ), and the appearance of aliphatic C–H stretches ( $2950\text{--}2850\text{ cm}^{-1}$ ) confirmed that polymerisation had taken place.

Pulsed plasma poly(vinylbenzaldehyde) coating showed relatively high water contact angle hysteresis and sliding angle values, Table 1. Impregnation with lubricants resulted in a significant decrease in the water contact angle hysteresis. Decanal and 2-methylundecanal also gave rise to low sliding angles ( $<5^\circ$ ). Although cinnamaldehyde and hexadecane reduced the sliding angles compared to the pulsed plasma poly(vinylbenzaldehyde)-only coating, they did not exhibit comparably low sliding angles.

Polypropylene cloth treated with 2-methylundecanal did not exhibit a slippery surface, Supporting Information Table S 8. Pulsed plasma poly(vinylbenzaldehyde) coated polypropylene cloth showed complete wetting in contact with water, which is likely due to the plasma polymer altering the surface wettability, therefore allowing the water to wick into the porous structure. Cinnamaldehyde and 2-methylundecanal impregnated pulsed plasma poly(vinylbenzaldehyde) coated polypropylene cloth both showed slippery surfaces. The water droplet sliding angles are not as low as for the same coatings on the flat PET substrate surface, Table 1—which is likely due to the dimpled, rough structure of the polypropylene cloth. Placing a  $100\ \mu\text{l}$  water droplet onto the pulsed plasma poly(vinylbenzaldehyde)–cinnamaldehyde coated polypropylene cloth for 4 h, and then a further 16 h produced no change in water droplet sliding angle values. Immersion of the coated sample into water for 16 h also yielded no change to the sliding angle.

Table S 8. Water droplet sliding angle values for pulsed plasma poly(vinylbenzaldehyde) (ppVBA) coated porous polypropylene (PP) cloth substrates. Values are reported as mean  $\pm$  standard deviation. † Samples display complete wetting / absorption of water droplets.

<b>Surface</b>	<b>Sliding Angle / °</b>
Polypropylene (PP) Cloth Untreated	36 $\pm$ 1
2-Methylundecanal–PP Cloth	29.3 $\pm$ 0.5
Cinnamaldehyde–PP Cloth †	-
ppVBA–PP Cloth *	-
ppVBA–2-Methylundecanal	12.3 $\pm$ 0.5
ppVBA–Cinnamaldehyde	15.3 $\pm$ 0.5
ppVBA–Cinnamaldehyde, 100 $\mu$ l water droplet, 4 h	14.3 $\pm$ 0.5
ppVBA–Cinnamaldehyde, 100 $\mu$ l water droplet, 20 h	14.7 $\pm$ 0.9
ppVBA–Cinnamaldehyde, immersion, 10 ml water, 16 h	14.3 $\pm$ 0.5

## 1.9 Pulsed Plasma Poly(Vinylbenzyl Chloride)

Vinylbenzyl chloride monomer displays the following characteristic infrared bands: C–H stretches ( $3095\text{--}2830\text{ cm}^{-1}$ ), aromatic ring summations ( $2000\text{--}1750\text{ cm}^{-1}$ ), vinyl C=C stretch ( $1630\text{ cm}^{-1}$ ), para-substituted aromatic ring stretches ( $1603\text{ cm}^{-1}$  and  $1511\text{ cm}^{-1}$ ), and Cl–CH<sub>2</sub> wag ( $1263\text{ cm}^{-1}$ ), Supporting Information Figure S 9.<sup>[6]</sup> Pulsed plasma deposited poly(vinylbenzyl chloride) retained the para-substituted aromatic ring stretches ( $1603\text{ cm}^{-1}$  and  $1511\text{ cm}^{-1}$ ), and Cl–CH<sub>2</sub> wag ( $1263\text{ cm}^{-1}$ ) infrared bands, demonstrating high structural retention and minimal cross-linking. The vinyl C=C stretch ( $1630\text{ cm}^{-1}$ ) disappeared indicating polymerisation had taken place.

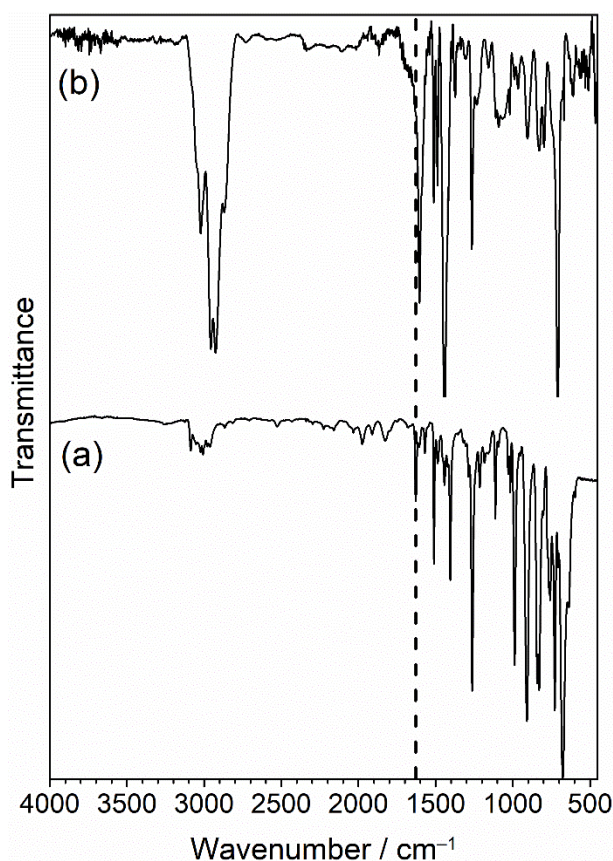


Figure S 9. Infrared spectra of: (a) vinylbenzyl chloride monomer (ATR); and (b) pulsed plasma poly(vinylbenzyl chloride) deposited onto silicon wafer (RAIRS, 55°). The dashed line corresponds to vinyl group absorbance ( $1630\text{ cm}^{-1}$ ).

Pulsed plasma poly(vinylbenzyl chloride) coated PET surface exhibited a relatively lower water contact angle hysteresis and sliding angle compared to the other styrene-type monomers investigated in this study, Table 1. Impregnation with

lubricants gave rise to slippery coatings. In particular, 2-methylundecanal lubricant produced a coating with excellent water repellency, with mean contact angle hysteresis and sliding angle values of 1°. Cinnamaldehyde lubricant did not give rise to a slippery surface.

## 1.10 Pulsed Plasma Poly(Perfluoroallylbenzene)

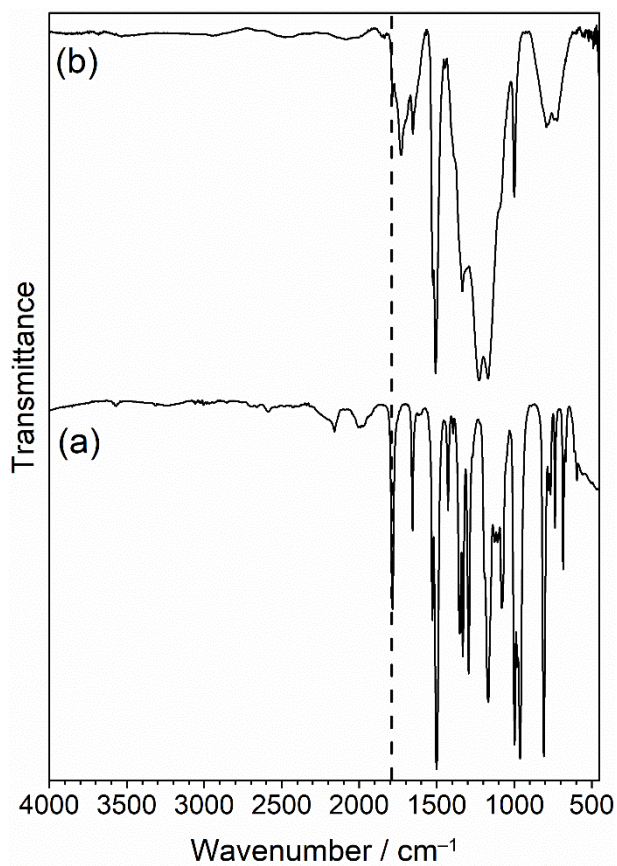


Figure S 10: Infrared spectra of: (a) perfluoroallylbenzene monomer (ATR); and (b) pulsed plasma poly(perfluoroallylbenzene) deposited onto silicon wafer (RAIRS, 55°). The dashed line corresponds to allyl group carbon–carbon double bond stretch absorbance (1787 cm<sup>-1</sup>).

## 1.11 Pulsed Plasma Poly(Vinylaniline)

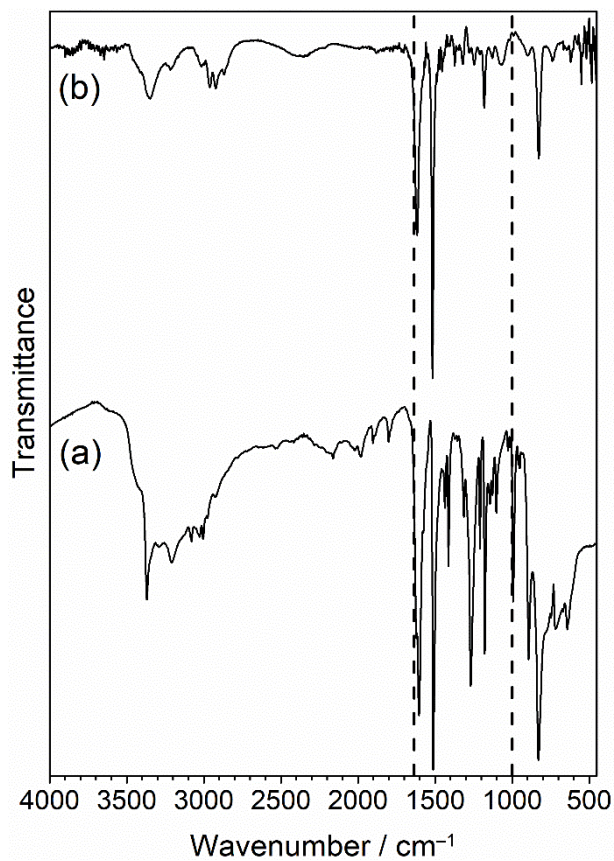


Figure S 11: Infrared spectra of: (a) vinylaniline monomer (ATR); and (b) pulsed plasma poly(vinylaniline) deposited onto silicon wafer (RAIRS,  $66^\circ$ ). The dashed lines correspond to vinyl group absorbances ( $1622 \text{ cm}^{-1}$  and  $994 \text{ cm}^{-1}$ ).

Table S9. Antibacterial tests for pulsed plasma poly(vinylaniline)–cinnamaldehyde coated PET film. Log<sub>10</sub> Reduction values are relative to the untreated substrate (average ± standard deviation).

Coating	Log <sub>10</sub> Reduction	
	<i>E. coli</i>	<i>S. aureus</i>
Cinnamaldehyde-Only (control)	0.12 ± 0.07	0.29 ± 0.07
Pulsed Plasma Poly(vinylaniline)-Only (Control)	0.19 ± 0.08	0.08 ± 0.09
Pulsed Plasma Poly(vinylaniline)–Cinnamaldehyde	8.04 ± 0.04	7.44 ± 0.03

## 2. VIDEOS

Video S 1. Ketchup applied to untreated glass vial (control). Several millilitres of ketchup are placed into the vial, and it is turned upside down. This video shows the ketchup moving very slowly from the vial upon turning upside down, and much of the ketchup remains stuck in the vial after a minute.

Video S 2. Ketchup applied to glass vial rinsed with decanal (control). Several millilitres of ketchup are placed into the vial, and it is turned upside down. This video shows the ketchup moving very slowly from the vial upon turning upside down, and much of the ketchup remains stuck in the vial after a minute.

Video S 3. Ketchup applied to pulsed plasma poly(vinylaniline) coated glass vial impregnated with decanal lubricant. Several millilitres of ketchup are placed into the vial, and it is turned upside down. The ketchup easily slides out of the vial in a matter of seconds, leaving none behind.

Video S 4. Honey applied to untreated glass vial (control). This video shows the honey moving slowly from the vial upon turning upside down, and much of the honey remains in the vial after a minute.

Video S 5. Honey applied to glass vial rinsed with 2-methylundecanal (control). This video shows the honey moving slowly from the vial upon turning upside down, and much of the honey remains in the vial after a minute.

Video S 6. Honey applied to pulsed plasma poly(vinylaniline) coated glass vial impregnated with 2-methylundecanal lubricant. Several millilitres of honey are placed into the vial, and it is turned upside down. This video shows the honey moves much faster out of the vial compared to the controls, and after a minute practically all the honey (aside from one small droplet) has left the vial.

### 3. REFERENCES

- [1] T.J. Bradley, W.C.E. Schofield, R.P. Garrod, J.P.S. Badyal, *Langmuir* **2006**, *22*, 7552.
- [2] C. Tarducci, E.J. Kinmond, J.P.S. Badyal, S.A. Brewer, C. Willis, *Chem. Mater.* **2000**, *12*, 1884.
- [3] P.S. Brown, T.J. Wood, W.C.E. Schofield, J.P.S. Badyal, *ACS Appl. Mater. Interfaces* **2011**, *3*, 1204.
- [4] D.O.H. Teare, C.G. Spanos, P. Ridley, E.J. Kinmond, V. Roucoules, J.P.S. Badyal, S.A. Brewer, S. Coulson, C. Willis, *Chem. Mater.* **2002**, *14*, 4566.
- [5] J.D. McGettrick, W.C.E. Schofield, R.P. Garrod, J.P.S. Badyal, *Chem. Vap. Depos.* **2009**, *15*, 122.
- [6] M. Wilson, R. Kore, A.W. Ritchie, R.C. Fraser, S.K. Beaumont, R. Srivastava, J.P.S. Badyal, *Colloids Surfaces A Physicochem. Eng. Asp.* **2018**, *545*, 78.